Research paper

Novel thiosemicarbazone derivatives containing indole fragment as potent and selective anticancer agent

Zhangxu He [1], Hui Qiao [1], Feifei Yang, Wenjuan Zhou, Yunpeng Gong, Xinhui Zhang, Haojie Wang, Bing Zhao, Liying Ma [**, 2], Hong-min Liu [***, 2], Wen Zhao [*, 2]

State Key Laboratory of Esophageal Cancer Prevention and Treatment, Key Laboratory of Advanced Pharmaceutical Technology, Ministry of Education of China, Co-innovation Center of Henan Province for New Drug R & D and Preclinical Safety, School of Pharmaceutical Sciences, Zhengzhou University, Zhengzhou, Henan, 450001, PR China

ABSTRACT

Potent and safe anticancer drugs research and development are still on the way to human health. In this report, a series of novel thiosemicarbazone derivatives containing indole fragment were designed and synthesized. Most compounds exhibited excellent antiproliferative activity against PC3, MGC803 and EC109 cell lines with low micromolar IC_{50} (0.14−12μM). Especially, compound **5j** can selectively inhibit PC3 cells in three tested tumor cells with IC_{50} value of 0.14 μM, which may be attributed to a synergistic effect after introducing indole fragment into the TSC structure. Meanwhile, compound **5j** displayed more selectivity in PC3 cells toward two normal WPMY-1 and GES-1 cell lines, compared to those of **3-AP** and **DPC**. We also found that **5j** can effectively inhibit PC3 cell proliferation, colonization and induce apoptosis. What's more, **5j** may significantly suppress migration and invasion by blocking the EMT process but had no effect on cell cycle. Collectively, our findings indicate that **5j** with structure of thiosemicarbazone containing indole may serve as a useful anticancer lead for further optimization and development.

© 2019 Elsevier Masson SAS. All rights reserved.

1. Introduction

Despite continued research efforts, cancer possessing extremely high fatality rate and low cure rate has posed the serious threat to human health [1]. To combat with cancer, efforts need to be concentrated on the design and synthesis of highly efficient antitumor agents with low toxicity to normal cells and tissues [2].

Thiosemicarbazone (TSC) as the privileged pharmacophore has received extensive attention from chemists and biologists because of possessing potential biological activity, including overcoming multidrug resistance, antituberculosis, antiviral, antifungal, antimalarial, and, most intriguingly, antineoplastic activity [3−8]. Antitumor activity of TSCs is mainly due to several factors, such as inhibition of tumor cell invasion and migration [9−11], chelating metal properties [12−14], interfering DNA synthesis [15,16], ROS generation [16], and affecting several crucial proteins [10]. To date, several TSC related drug candidates have been in clinical trial. 3-AP (Fig. 1), a metal chelating agent, is currently in phase II clinical trial. Compared to 3-AP, COTI-2 and DPC (Fig. 1), another TSC-containing drugs, improved the activity and selectivity toward tumor cells [7,12,13]. Although this family of compounds was extensively reported, highly selective TSCs with strong cytotoxicity against cancer cells and less side effect remain to be discovered (see Fig. 2).

Recently, we have reported a series of TSC derivatives like **5n (TS-1)** that showed acceptable antiproliferative activity and could suppress migration of MGC803 cells to some extent [17]. In addition, compounds containing indole fragment displayed extensive biological activity of which inhibition of tumor cells metastasis stood out [18−22]. For example, Panobinostat, approved in 2015, shows the ability to inhibit invasion and metastasis and significantly antiproliferative effect [23,24]. Inspired by biological profile of indole and in continuation with our previous work on the identification of novel TSC derivatives, we herein report the design and synthesis of novel TSC derivatives containing indole and their
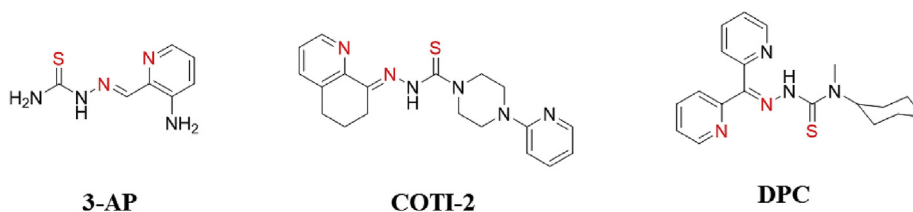
Fig. 1. Representative compounds with TSC structure in the clinical trial.
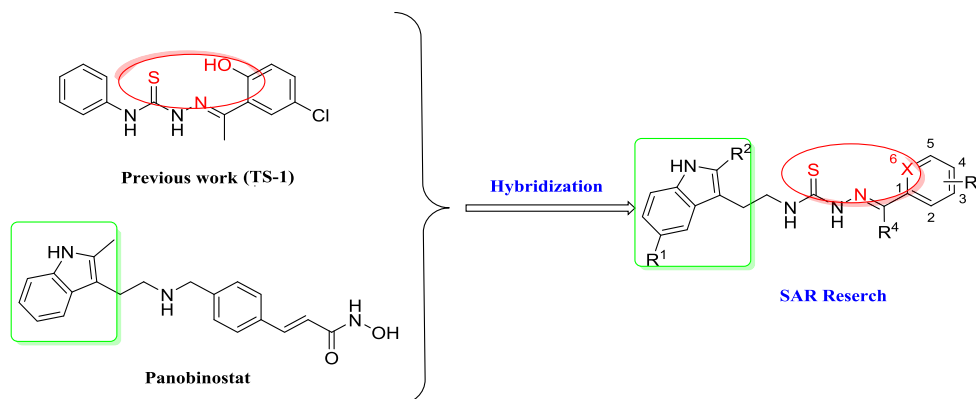

Fig. 2. Design of novel thiosemicarbazone derivatives containing indole.

underlying mechanisms of antiproliferative activity (Fig. 2).

2. Results and discussion

2.1. Chemistry

The desired TSC derivatives were provided by a synthetic three-step route as shown in Scheme 1. At first, various aliphatic and aromatic amines **1a-k** was reacted with carbon disulfide under basic condition, followed by the addition of 4-dimethylaminopyridine (DMAP) and di-*tert*-butyl decarbonate (Boc$_2$O) to provide the corresponding products **2a-k** in 48−66% yields [25]. Then, after treatment of **2a-k** with an excess of hydrazine hydrate in dichloromethane, compounds **3a-k** were afforded

in 65−85% yields. The compounds **4a-f** or **5a-v** could be derived from a Schiff base condensation reaction between **3a-k** and appropriate aldehyde or ketone with the presence of acetic acid in ethanol, yields ranging from 45 to 85% [26,27].

The full characterization of all thiosemicarbazones was permitted by ^{1}H NMR, ^{13}C NMR and high-resolution mass (HRMS). The compounds **4a-f** and **5a-v** exhibited in ^{1}H NMR spectra at δ 6.75−8.60 ppm matching to protons correlated to the phenyl group, moreover a singlet peak in the range of δ 7.25−8.25 ppm attributed to azomethine group (-CH=N-), which was comparable to the literature involving TSCs [28]. In addition, N−H indole ring showed a singlet peak in the range of δ 10.75−11.20 ppm and N−H hydrazine proton displayed chemical shifts at δ 8.60−11.75 ppm region. Finally, the other signals related to thiosemicarbazone, such
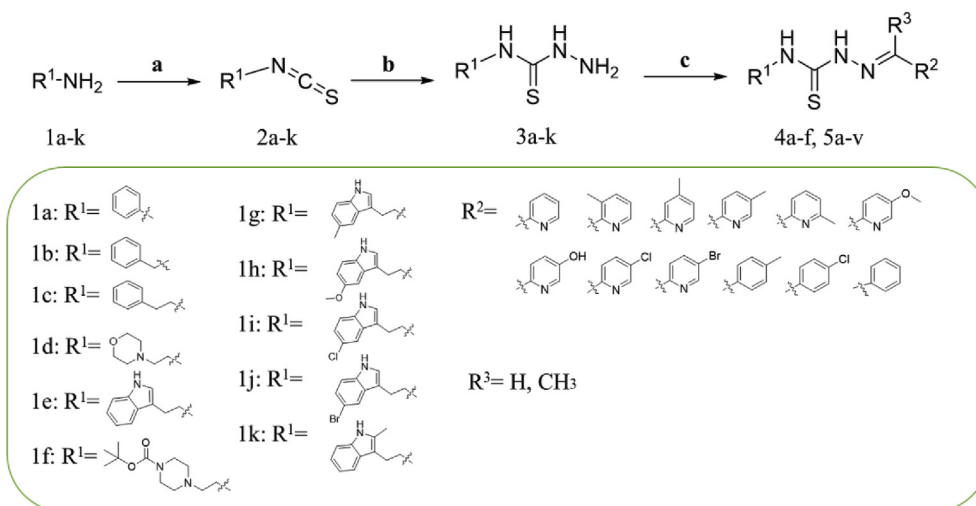
Scheme 1. Reagents and conditions: (a) (1) CS$_2$, triethylamine, EtOH, rt; (2) Boc$_2$O, DMAP, EtOH, rt; (b) hydrazine hydrate, dichloromethane, rt; (c) appropriate aldehyde or ketone, acetic acid, EtOH, rt.

as the protons of alkane occurred between δ 2.25 and 4.80 ppm. In the ^{13}C NMR spectra, the chemical shift of C=N group occurred in the range of δ 140.22−153.84 ppm and C=S group appeared at the region of δ 175.93−177.90 ppm, both in accordance with the reports [28−30]. These data markedly confirmed the formation of **4a-f** and **5a-v**.

The compounds **4a-f** and **5a-v** could exist in either *E* or *Z* isomeric form because of azomethine (-CH=N-). We continued exploring the predominant isomers of our derivatives. From ^{1}H NMR spectra, it is possible to detect a single peak as −CH=N- signal between δ 7.25 and 8.25 ppm. As the most outstanding compound, **5j** was chosen to explain the isomerism. A single spot was observed in thin layer chromatography (TLC) and the purity of **5j** was 99.04%, determined by reverse-phase high-performance liquid chromatography (HPLC) analysis (See supplementary material). The above results showed the presence of a single isomeric form. In order to further confirm the stereochemistry more precisely, the NOESY experiment of **5j** was performed. The NOESY spectra clearly displayed the spatial correlation between azomethine (-CH=N-) at δ 7.25 ppm and the hydrogen of =N−NH at δ 11.71 ppm, which existed only in the *E* isomer because of the appropriate intramolecular H−H distance (See supplementary material). These results indicated that the *E* isomer was generated, which was consistent with NOESY spectrum of *E*-thiosemicarbazone displayed in the literature [28,31,32].

2.2. Evaluation of biological activity

2.2.1. Anti-proliferative activity

Vandresen et al., reported that TSC derivatives exhibited considerable inhibitory effects on human prostate cancer cells (PC3), gastric cancer cells (MGC803) and esophageal cancer cells (EC109) [17,33,34]. Therefore, we evaluated the antiproliferative activity of synthesized compounds **4a-f** and **5a-v** toward the three cell lines by using the MTT assay. **3-AP** and **DPC** were used as the positive controls. Based on previous work, **4a-c** were firstly synthesized. As Table 1 showed that the length of the carbon chain at the R^1 position had a weak effect on the activity against PC3 cells. However, the compounds displayed better selectivity for PC3 comparing to MGC803 cells with the carbon chain extended, the selectivity index 1 (SI$_1$) of **4a**, **4b** and **4c** were 5.69, 9.42 and 16.6 respectively [35]. The antiproliferation activity of compounds **4d-f** towards PC3 cells suggested that when R^1 position was a hydrophilic heterocycle, the compounds displayed weak inhibitory activity against the three cells screened. To our delight, **4e** (IC$_{50}$ = 0.60 ± 0.22 μM) with the indole fragment had more markedly antiproliferative effect, comparing to **4c** (IC$_{50}$ = 0.98 ± 0.10 μM) toward PC3 cells.

Compounds **5a-v** were synthesized to improve antiproliferative activity and selectivity based on **4e**'s indole group. As shown in Table 1, the antitumor activity of compounds **5a** and **5b** bearing a methyl group and methoxy group respectively in indole ring showed no obvious difference with their parent compound **4e** toward PC3 cell lines. What's more, compounds with an electron-withdrawing substitute, namely, **5c** (IC$_{50}$ = 0.28 ± 0.04 μM) or **5d** (IC$_{50}$ = 0.35 ± 0.02 μM), suggested better potency than **4e** with an electron-donating substitute. These results suggested that electron-withdrawing groups at the 5-position of the indole may be more favorable for inhibitory activity than electron-donating groups. In addition, the results exhibited after methyl was added at the 2-position of the indole like **5e**, the activity was inferior than **4e** toward PC3 cells. To investigate the effect of R^2 position on activity, **5f-j** were synthesized by introducing different substitutes at the 4-position of pyridine ring. When the C-4 of pyridine ring was methyl, the activity had been slightly improved, such as **5c**

(IC$_{50}$ = 0.28 ± 0.04 μM) vs **5j** (IC$_{50}$ = 0.14 ± 0.02 μM). Interestingly, when the 4-position of the pyridine ring was other substitutes (hydroxyl, methoxy, chlorine, bromine), the activity decreased compared to **5c** against PC3 cells. These results implied that the presence of the methyl group at the pyridine ring was critical for cytotoxic activity. **5k-m** were prepared by changing the position of the methyl group on the pyridine ring. The results presented that the C-2, C-3, and C-4 on the pyridine ring had slight effect on the activity toward PC3 cells. However, the activity of compounds was significantly decreased toward PC3, MGC803 and EC109 cells when methyl group was added to the 5-position of pyridine ring (**5j**, **5k** or **5l** vs **5m**). Furthermore, **5l** (IC$_{50}$ = 0.33 ± 0.03 μM) had better antiproliferative activity than **5j** (IC$_{50}$ = 2.94 ± 0.47 μM) for MGC803 cells, but **5j** showed 21 times better selectivity between PC3 and MGC803 cells. By comparing the activity of **5n** and **5c** on PC3 cells, the methyl group at the R^3 position was not conducive to increase activity. Similarly, **5o** (IC$_{50}$ = 0.72 ± 0.14 μM) and **5j** (IC$_{50}$ = 0.14 ± 0.02 μM), **5p** and **5c** also displayed this phenomenon toward PC3 cells. The activity of **5r-v** almost disappeared toward three tumor cells after replacing the pyridyl at the R^2 position with phenyl, suggesting that pyridine ring, present in majority of our compounds, similar to 3-AP, may improve the metal chelation property to further increase their toxicity, which was in accordance to the literature [5,7]. The selectivity index of all compounds between PC3 and MGC803 or EC109 cell lines was also calculated and the results indicated most derivatives could selectively inhibit PC3 cell lines as shown Table 2 [35]. What's more, the compounds with selectivity were also evaluated against PC3 cell lines for 24 h and 48 h in Table 3.

Based on these data, we try to explore the efficacy of all compounds in human normal prostate cell (WPMY-1) and human gastric mucosal epithelial cells (GES-1). The results were shown in Table 1. Surprisingly, most of derivatives displayed obvious selectivity between cancer cells and normal cells. Especially, **5j** suggested more selectivity in PC3 cells toward two normal cell lines, compared to those of **3-AP** and **DPC** as shown in Table 4. What's more, **5j** with an IC$_{50}$ value of 0.14 μM against PC3 cells displayed about 4-fold more potent than **3-AP** (IC$_{50}$ = 0.56 ± 0.03 μM) and equivalent inhibitory activity with that of **DPC** (IC$_{50}$ = 0.12 ± 0.02 μM). The compound **5j** also showed significant advantages in terms of activity and selectivity compared to cisplatin. This series of TSC derivatives containing indole scaffold may have great reference value for the future development of anticancer drugs. Fig. 3 shows the summary illustration for structure-activity relationship (SAR) study of target derivatives.

2.2.2. Clone assay

As shown in Fig. 4A, compound **5j**, with excellent anti-proliferative activity and selectivity, inhibited PC3 cells proliferation in a time- and concentration-dependent manner. Favorable anti-proliferative activity of compound **5j** against PC3 cells led us to further explore the effect on cell colony formation. Colony formation assay represents the ability of cancer cells to grow and form foci [36]. The results displayed that **5j** was able to inhibit the colony formation of PC3 cells dose-dependently from Fig. 4B and C. What's more, as the concentration of **5j** increased, the colonies by the compound-added group became smaller and fewer, compared with the control group. Evidently, colony formation was almost completely suppressed at 200 nM.

2.2.3. Cell apoptosis assay

Apoptosis as programmed cell death can control most cell death in biological processes [37]. To investigate the ability of compound **5j** in apoptosis, Hoechst 33342 staining was performed using PC3 cells. After 48 h treatment with compound **5j**, the typical changes in

Table 1
The antiproliferative activity of compounds **4a-f** and **5a-v** against the tested cancer cell lines.

Compd.	R^1	R^2	R^3	IC$_{50}$ (µM)[a]				
				PC3	MGC803	EC109	WPMY-1	GES-1
4a			H	1.75 ± 0.24	9.96 ± 0.99	3.02 ± 0.48	0.67 ± 0.18	0.32 ± 0.05
4b			H	0.97 ± 0.01	9.14 ± 0.96	7.15 ± 0.85	2.87 ± 0.46	3.12 ± 0.49
4c			H	0.98 ± 0.10	16.28 ± 1.21	5.57 ± 0.74	1.17 ± 0.72	0.82 ± 0.08
4d			H	19.53 ± 1.29	22.31 ± 1.35	24.26 ± 1.38	9.43 ± 0.87	13.20 ± 1.12
4e			H	0.60 ± 0.22	7.78 ± 0.89	4.47 ± 0.65	7.47 ± 0.87	9.88 ± 0.99
4f			H	8.66 ± 0.94	12.24 ± 1.01	15.73 ± 1.19	7.61 ± 0.75	9.24 ± 0.97
5a			H	0.93 ± 0.03	2.81 ± 0.44	12.21 ± 1.09	4.84 ± 0.26	5.21 ± 0.72
5b			H	0.56 ± 0.03	3.74 ± 0.57	3.10 ± 0.49	2.23 ± 0.35	3.32 ± 0.52
5c			H	0.28 ± 0.04	0.54 ± 0.28	2.56 ± 0.41	2.16 ± 0.26	2.38 ± 0.37
5d			H	0.35 ± 0.02	1.49 ± 0.17	5.04 ± 0.70	0.52 ± 0.29	2.05 ± 0.31
5e			H	1.07 ± 0.03	4.20 ± 0.62	3.51 ± 0.54	3.99 ± 0.42	4.81 ± 0.68
5f			H	0.34 ± 0.25	0.89 ± 0.05	6.44 ± 0.81	1.17 ± 0.07	3.47 ± 0.54
5g			H	0.67 ± 0.18	7.08 ± 0.85	9.32 ± 0.97	4.75 ± 0.44	4.11 ± 0.61
5h			H	0.52 ± 0.28	6.86 ± 0.84	10.64 ± 1.03	2.17 ± 0.07	3.75 ± 0.57
5i			H	0.51 ± 0.03	2.23 ± 0.35	8.23 ± 0.91	2.13 ± 0.33	1.58 ± 0.20
5j			H	0.14 ± 0.02	2.94 ± 0.47	3.99 ± 0.60	9.85 ± 0.26	9.23 ± 0.96
5k			H	0.16 ± 0.02	2.24 ± 0.35	0.97 ± 0.01	1.01 ± 0.04	1.62 ± 0.21
5l			H	0.19 ± 0.02	0.33 ± 0.03	4.14 ± 0.62	1.19 ± 0.07	1.99 ± 0.30
5m			H	1.09 ± 0.03	10.77 ± 1.03	>20	9.52 ± 0.60	8.53 ± 0.81
5n			-CH$_3$	0.40 ± 0.03	2.82 ± 0.45	2.57 ± 0.41	2.06 ± 0.31	1.88 ± 0.27

Table 1 (*continued*)

Compd.	R^1	R^2	R^3	IC$_{50}$ (μM)[a]				
				PC3	MGC803	EC109	WPMY-1	GES-1
5o			-CH$_3$	0.72 ± 0.14	2.48 ± 0.39	5.52 ± 0.74	1.06 ± 0.02	2.21 ± 0.35
5p			-CH$_3$	0.71 ± 0.15	>20	>20	2.69 ± 0.43	3.52 ± 0.55
5q			-CH$_3$	1.53 ± 0.18	15.94 ± 1.20	9.36 ± 0.97	2.51 ± 0.39	0.51 ± 0.02
5r			H	19.33 ± 1.23	>20	>20	>20	>20
5s			H	>20	>20	>20	>20	>20
5t			H	>20	>20	>20	>20	>20
5u			-CH$_3$	18.87 ± 1.27	>20	>20	>20	11.66 ± 1.06
5v			-CH$_3$	>20	>20	>20	>20	>20
Cisplatin	–	–	–	5.44 ± 0.21	1.82 ± 0.21	4.21 ± 0.23	17.25 ± 0.09	19.02 ± 0.07

[a] Inhibitory activity was assayed by exposure various concentrations of the tested compounds for 72 h to substance and expressed as concentration required to inhibit tumor cell proliferation by 50% (IC$_{50}$). Data are presented as the means ± SDs. All experiments were carried out at least three independent times.

apoptotic morphology were observed, including chromatin shrinkage, cell rounding and formation of apoptotic bodies (Fig. 5A) [38]. In addition, Annexin V-FITC/PI double staining flow cytometry method was also used. We found that compound **5j** can induce PC3 cell apoptosis dose-dependently (Fig. 5B). Apoptosis induction is mediated via the intrinsic pathway with the elevation of total reactive oxygen species [39]. In order to further explore the potential mechanism, we examined the intracellular ROS, using the reactive oxygen assay. The results indicated the compound **5j** can induce apoptosis, which was not affected by reactive oxygen mechanism (supporting information).

The expression of apoptosis-related proteins was also detected. As shown in Fig. 5C, the expression of pro-apoptotic proteins Bax was significantly increased, while anti-apoptotic protein Bcl-2 was down-regulated. What's more, we evaluated the effect of compound **5j** on the activity of caspase 3/9 and PARP. The compound **5j** had down-regulated the pro-caspase9 and PARP, meanwhile the expression of cleaved caspase 9/3 and cleaved PARP were significantly increased concentration-dependently. Furthermore, expression level of P53 was not significantly changed after adding different concentrations of compound **5j**. These results collectively indicated the compound **5j** could induce PC3 cell apoptosis at least partially via the mitochondrial death pathway.

2.2.4. Cell migration assay

The tumor cell invasion and metastasis are undoubtedly the great challenge for the treatment of tumors. Recently, publication has showed that abnormal epithelial-mesenchymal transition (EMT) activation is closely related to the invasion of prostate cancer cells [40]. In consideration of the outstanding anti-proliferative activity of **5j** against PC3 cells, we investigated whether compound **5j** can effectively inhibit the migration and invasion of PC3 cells. As shown in Fig. 6A, treatment of PC3 cells with **5j** at indicated concentrations significantly suppressed the wound healing concentration-dependently.

In addition, the further transwell assay (Fig. 6B) demonstrated that compound **5j** could inhibit the migration ability of PC3 cells in a dose-dependent manner. The expression of mesenchymal cells' biomarkers N-Cadherin and epithelial cells' biomarkers E-Cadherin and β-catenin are important indicator of cell migration. Western Blot analysis (Fig. 6C) suggested that **5j** up-regulated the expression of E-Cadherin, while N-Cadherin and β-catenin were down-regulated. These results indicated that the compound **5j** may inhibit migration of PC3 cells in a concentration-dependent manner by blocking the EMT process.

2.2.5. Cell cycle analysis

Cell cycle arrest is a marker closely related to cell proliferation inhibition [41]. To better explain the antiproliferative activity of compound **5j** against PC3 cells, cell-cycle analysis was carried out by flow cytometry (Fig. 7). After treatment of PC3 cells with **5j** for 48 h at indicated concentrations (0, 100, 200, 400 nM), we found that **5j** had almost no effect on cell cycle (Fig. 7A), which was significantly different from that of the TSC compound **TS-1** reported previously, what led to S-phase arrest pattern toward MGC-803 cells in a dose-dependent manner [41]. To explore the impact of time on PC3 cell cycle, the time of **5j** and PC3 cells co-incubation was extended to 72 h. Unfortunately, PC3 cell cycle was not affected by **5j** (Fig. 7B). The effect of compounds **5j** and **TS-1** on the cell cycle of MGC803 and PC3 cells was also evaluated respectively. The results showed that **5j** didn't arrest the cell cycle of MGC803 cells and **TS-1** caused an obvious S arrest in a dose-dependent manner with concomitant decrease in terms of the number of cells in other phases of PC3 cell cycle (Fig. 7C and D). We speculated that structural difference in drugs may lead to changes in biological function. Jamerson et al., reported a series of thiosemicarbazone derivatives containing indole but no pyridyl groups, of which the representative compound **2b** could effectively induce G2/M arrest [28]. In

Table 2
The selectivity index of all compounds between PC3 and MGC803 or EC109 cell lines.

Compd.	R¹	R²	R³	Selectivity index	
				SI₁[a]	SI₂[b]
4a			H	5.69	1.73
4b			H	9.42	7.37
4c			H	16.60	5.68
4d			H	1.14	1.24
4e			H	12.97	7.45
4f			H	1.41	1.82
5a			H	3.02	13.13
5b			H	6.68	5.54
5c			H	1.93	9.14
5d			H	4.26	14.40
5e			H	3.93	3.28
5f			H	2.62	18.94
5g			H	10.57	13.91
5h			H	13.19	20.46
5i			H	4.37	16.14
5j			H	21.00	28.50
5k			H	14.00	6.06
5l			H	1.74	21.79
5m			H	9.88	18.35
5n			-CH₃	7.05	6.43

Table 2 (continued)

Compd.	R¹	R²	R³	Selectivity index	
				SI₁[a]	SI₂[b]
5o			-CH₃	3.44	7.67
5p			-CH₃	28.17	28.17
5q			-CH₃	10.42	6.12
5r			H	1.03	1.03
5s			H	1.00	1.00
5t			H	1.00	1.00
5u			-CH₃	1.06	1.06
5v			-CH₃	1.00	1.00

[a] The selectivity index (SI₁) was calculated as IC₅₀ (MGC803)/IC₅₀ (PC3).
[b] The selectivity index (SI₂) was calculated as IC₅₀ (EC109)/IC₅₀ (PC3).

Table 3
Inhibitory activity of selective compounds against PC3 cell lines for 24, 48 and 72 h.

Compd.	IC₅₀ (μM)[a]		
	24 h	48 h	72 h
5f	>20	4.21 ± 0.62	0.34 ± 0.25
5h	>20	6.01 ± 0.78	0.52 ± 0.28
5l	7.51 ± 0.87	1.78 ± 0.25	0.19 ± 0.02
5m	15.23 ± 1.18	5.15 ± 0.71	1.09 ± 0.03
5p	>20	6.48 ± 0.81	0.71 ± 0.15

[a] Inhibitory activity was assayed by exposure various concentrations of the tested compounds for 24 h, 48 h and 72 h to substance and expressed as concentration required to inhibit tumor cell proliferation by 50% (IC₅₀). Data are presented as the means ± SDs. All experiments were carried out at least three independent times.

addition, 3-AP, consist only of thiosemicarbazone and pyridine, resulted in an extensive G₁/S-phase cell cycle arrest. Our thiosemicarbazone derivative **5j** contains both hydrazine and pyridyl group, which may cause **5j** to lose the regulatory function of the cell cycle. The detail mechanism needs to be further examined in our future study.

3. Discussion and conclusions

In the current investigation, a series of novel thiosemicarbazone derivatives containing indole fragment were designed and synthesized. Most of the compounds displayed potent antiproliferative activity against PC3, MGC803 and EC109 cell lines. The SAR study showed that both the electron-withdrawing group at the 5-position of the indole and electron-donating substitute at the 4-position of the pyridine ring were critical for antiproliferative activity and selectivity. The representative compound **5j** exhibited highly potent antiproliferative activity toward the tested cancer cell lines and less toxicity against the normal WPMY-1 and GES-1 cell lines than 3-AP, cisplatin and DPC.

Table 4
Inhibitory activity of compounds **5j**, **3-AP** and **DPC** against PC3 and two normal cell lines.

Comp.	PC3	WPMY-1		GES-1	
	IC$_{50}$ (μM)[a]	IC$_{50}$ (μM)[a]	Fold selectivity	IC$_{50}$ (μM)[a]	Fold selectivity
5j	0.14 ± 0.02	9.85 ± 0.26	70.4	12.29 ± 1.09	87.8
3-AP	0.56 ± 0.03	4.96 ± 0.02	8.9	5.60 ± 0.40	10
DPC	0.12 ± 0.02	0.71 ± 0.15	5.9	0.44 ± 0.03	3.7
Cisplatin	5.44 ± 0.21	17.25 ± 0.09	3.2	19.02 ± 0.07	3.5

[a] Inhibitory activity was assayed by exposure various concentrations of the tested compounds for 72 h to substance and expressed as concentration required to inhibit tumor cell proliferation by 50% (IC$_{50}$). Data are presented as the means ± SDs. All experiments were carried out at least three independent times.
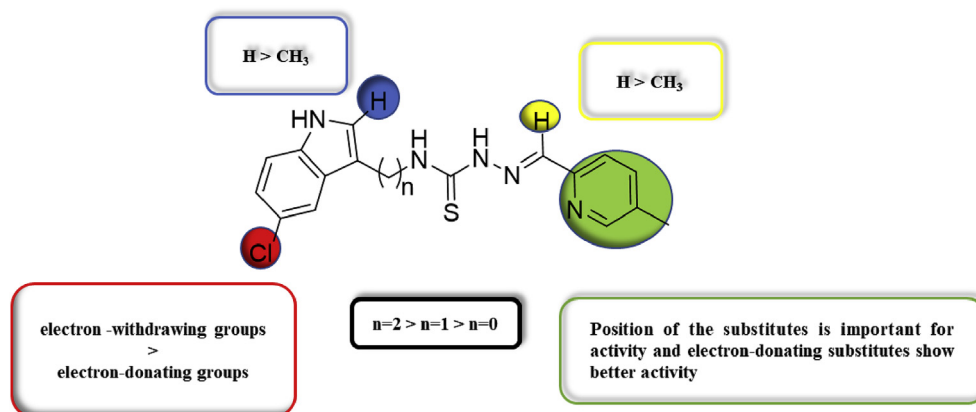
Fig. 3. The summary for SAR studies of the indicated compounds in Scheme 1.
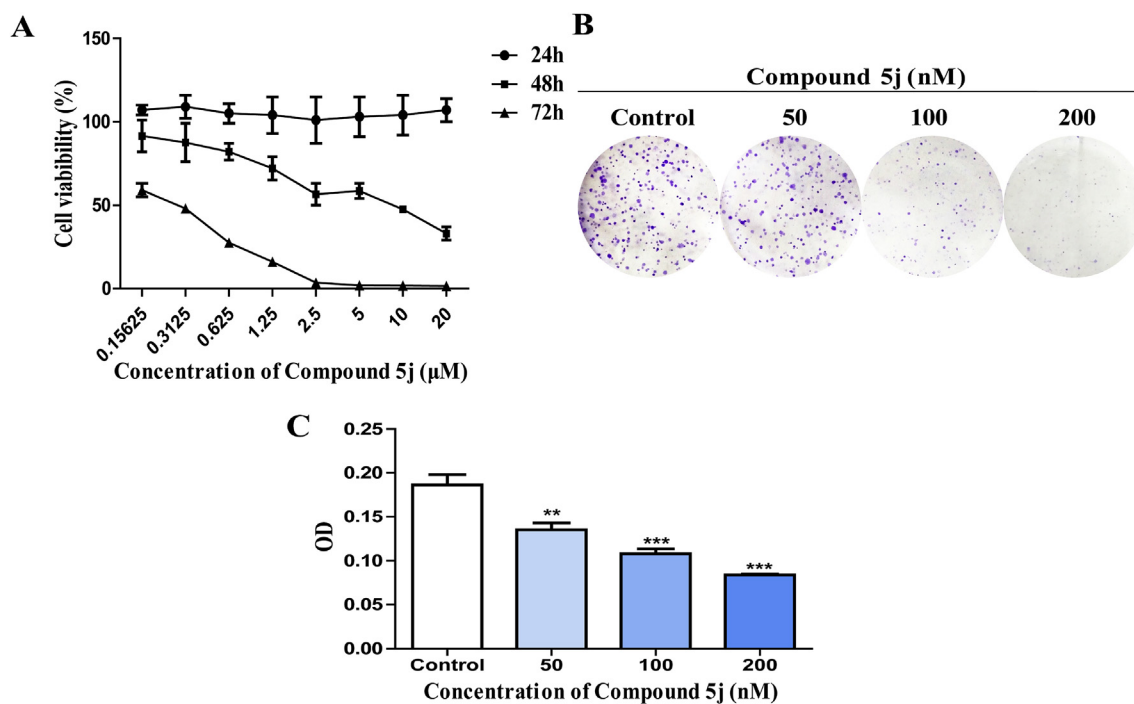
Fig. 4. (A) PC3 cells were treated with compound **5j** at the indicated concentrations for 24 h, 48 h and 72 h. Cell viability was determined by MTT. (B) The colony formation of PC3 cells after treated with compound **5j** for 7 days. (C) The rate of inhibition was quantified by measuring the absorbance of 570 nm. The dates were represented as the Mean ± SD. All experiments were performed at least three times. *$p < 0.5$, **$p < 0.01$, ***$p < 0.001$ compared with the control.

Compound **5j** was chose for further exploring the mechanisms underlying antiproliferative activity. Colony formation assay showed that **5j** can inhibited colony formation concentration-dependently. What's more, we certified that compound **5j** could induced apoptosis by Hoechst 33342 staining and Annexin V-FITC/PI dual staining assays. Extrinsic pathway and intrinsic pathway as the core pathways involve in inducing apoptosis. Extrinsic pathway mentions DR-mediated pathway and the intrinsic pathway is a
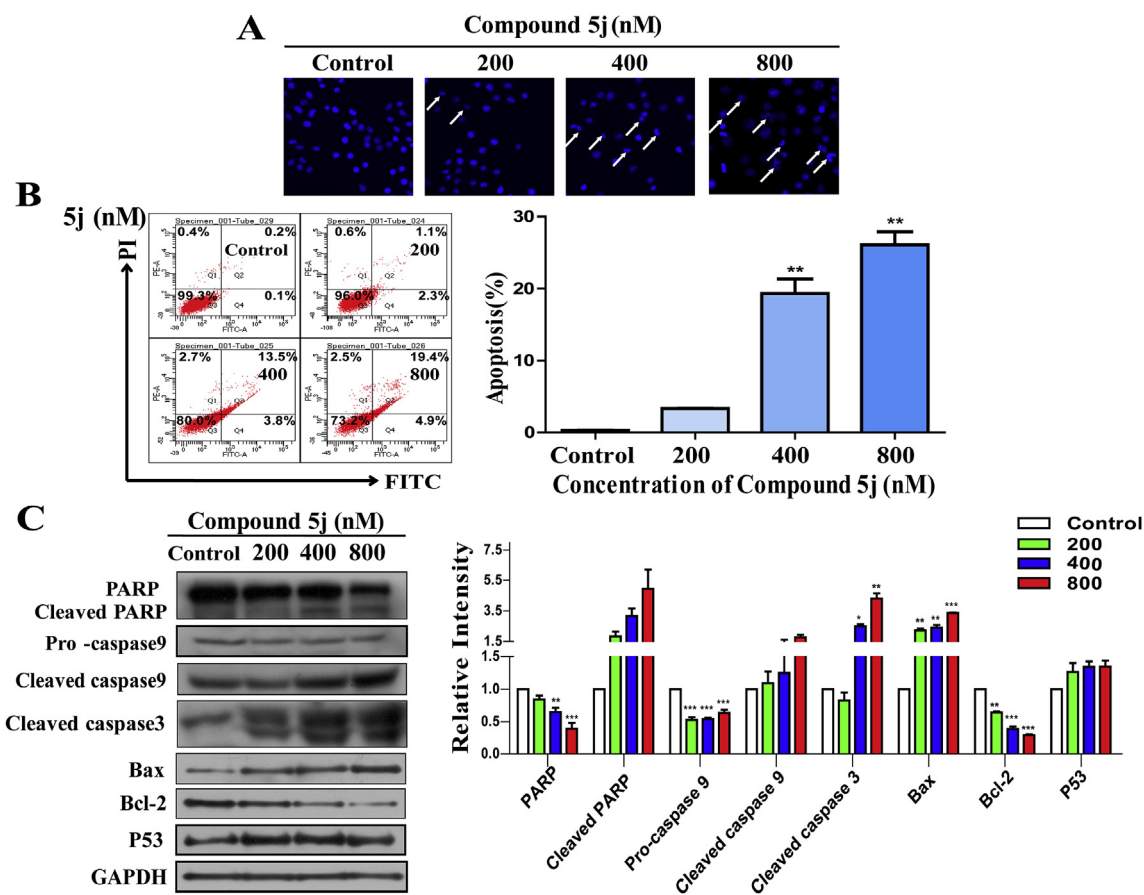
Fig. 5. Compound **5j** induced PC3 cell apoptosis and possible mechanisms. (A) PC3 cells were treated with compound **5j** for 48 h and then stained with Hoechst 33342 to reflect changes in cell morphology. (B) Apoptotic PC3 cells were analyzed with Annexin V-FITC/PI double staining. Quantitative analysis of apoptosis rates by flow cyometry. (C) Expression of apoptosis-related proteins including Pro-caspase9, PARP, Cleaved caspase9/3, Cleaved PARP, Bax, Bcl-2 and P53. The GAPDH was used as a control. The dates were represented as the Mean ± SD. All experiments were performed at least three times. *p < 0.5, **p < 0.01, ***p < 0.001 compared with the control.

mitochondrial-mediated pathway [42]. Western blot analysis indicated that treatment of PC3 cells with **5j** caused an increase of cleaved PARP and cleaved caspases 3 and 9, suggesting that **5j** might induce apoptosis at least partially via the mitochondrial death pathway. In addition, apoptosis is mediated mainly via the intrinsic pathway with the elevation of total reactive oxygen species [39], but the level of total ROS wasn't affected by compound **5j**. The molecular mechanism how compound **5j** targets and induces apoptosis warrants to be further investigated.

Collectively, **5j** can markedly inhibit colony formation, induce apoptosis and suppress migration and invasion. Our findings suggest **5j** with structure of thiosemicarbazone containing indole may serve as a useful anticancer lead for further optimization and development.

4. Experimental section

4.1. General

Reagents and solvents were purchased from commercial sources and used without further purification. Thin-layer chromatography (TLC) was carried out on the glass pane that painted with silica gel, visualized by 254 nm ultraviolet lamp. Melting points were determined on a WRS-1A digital melting point apparatus and are uncorrected. ^{1}H NMR and ^{13}C NMR spectra were recorded on a Bruker 400 MHz and 100 MHz spectrometer respectively. High resolution mass spectra (HRMS) were recorded on a Waters

Micromass Q-T of Micromass spectrometer by electrospray ionization (ESI). The purity of the compound **5j** was determined by reverse-phase high-performance liquid chromatography (HPLC) analysis. The signal was monitored at 287 nm with a UV detector. A flow rate of 1.0 mL/min was used with a mobile phase of MeOH in H_2O (90:10, v/v).

4.2. General procedure for the synthesis of compounds(2a-k)

One pot method was adopted for synthesis of **2a-k**. Firstly, in a 50 ml round-bottom flask, appropriate primary amine **1a-k** (3.125 mmol), triethylamine (6.25 mmol) and CS_2 (6.25 mmol) were dissolved in ethanol (15 mL). The reaction mixture was stirred for 3 h at room temperature. Upon completion of the reaction, di-*tert*-butyl decarbonate (8.5 mmol), dissolved in absolute ethanol, was added followed by the immediate addition of a catalytic amount of 4-dimethylaminopyridine (0.425 mmol). After the reaction mixture was kept for further 30 min at room temperature, the solvent was distilled off under reduced pressure, and the residue was purified by column chromatography (petroleum ether/ethyl acetate = 4:1) to afford the corresponding **2a-k** in 48–66% yield.

4.3. General procedure for the synthesis of compounds(3a-k)

To a solution of **2a-k** (10 mmol) in dichloromethane (25 mL) was injected hydrazine hydrate (30 mmol) portion-wise. After the mixture was stirred at room temperature for 2 h, the formed
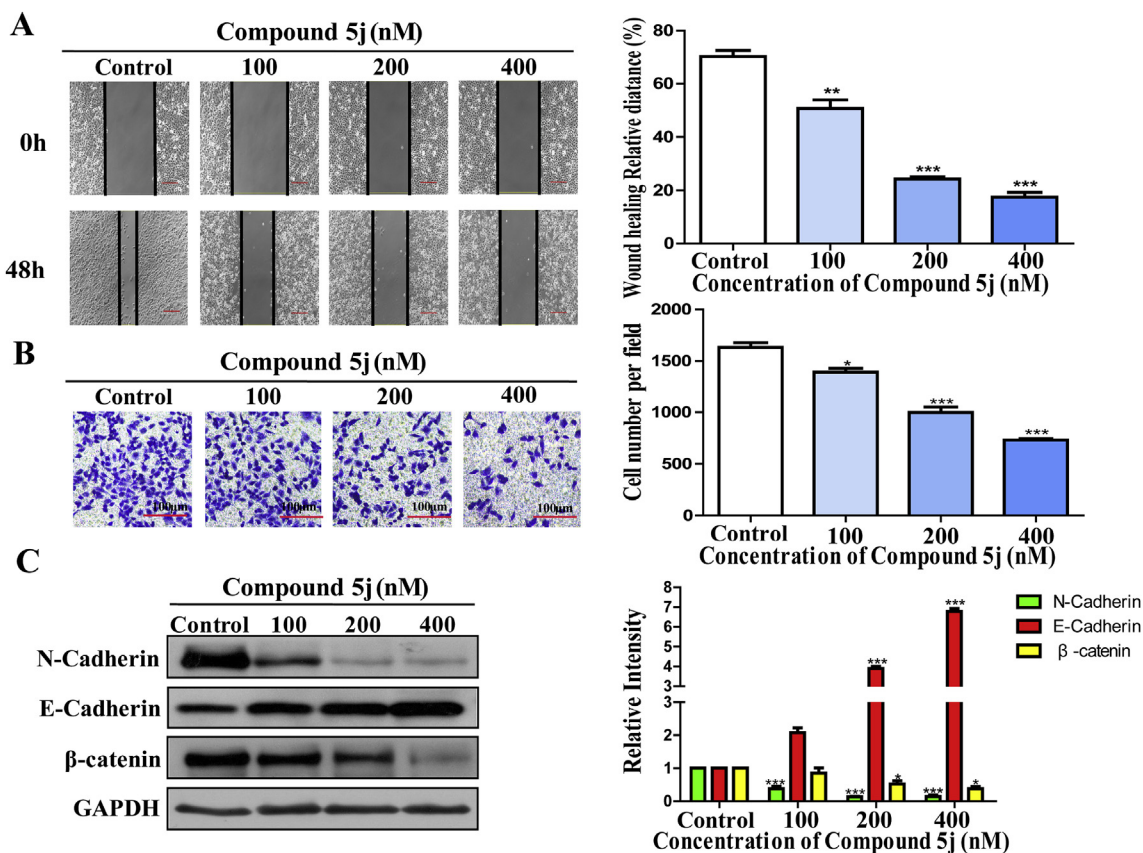
Fig. 6. Compound **5j** suppressed the migration of PC3 cells. (A) Wound healing assay. (B) PC3 cells were treated with compound **5j** at the indicated concentrations for 48 h, then used transwell assay to reflect the anti-migration ability of compound **5j**. Quantitative analysis of cell numbers. (C) Expression of N-Cadherin, E-Cadherin and β-catenin were quantified after treatment of compound **5j** for 48 h. The dates were represented as the Mean ± SD. All experiments were performed at least three times. *p < 0.5, **p < 0.01, ***p < 0.001 compared with the control.

precipitation was filtered, and the left residue was washed with dichloromethane to give compounds **3a-k** as solid in 65−85% yield.

4.3.1. N-Phenylhydrazinecarbothioamide(**3a**)

White solid, yield 80%. ^{1}H NMR (400 MHz, DMSO-d_6, δ, ppm) δ 9.69 (s, 1H, −NH−), 9.12 (s, 1H, −NH−), 7.65 (d, J = 6.2 Hz, 2H, Ar−H), 7.29 (t, J = 7.9 Hz, 2H, Ar−H), 7.09 (t, J = 7.3 Hz, 1H, Ar−H), 4.79 (s, 2H, −NH$_2$). ^{13}C NMR (100 MHz, DMSO-d_6, δ, ppm) δ 179.32, 139.25, 128.00, 124.01, 123.45. HR-MS (ESI), calcd. C$_7$H$_9$N$_3$S, [M+Na]$^+$$m/z$: 190.0415. found: 190.0416.

4.3.2. N-benzylhydrazinecarbothioamide(**3b**)

White solid, yield 84%. ^{1}H NMR (400 MHz, DMSO-d_6, δ, ppm) δ 8.73 (s, 1H, −NH−), 8.28 (s, 1H, −NH−), 7.44−7.10 (m, 5H, Ar−H), 4.72 (d, J = 6.1 Hz, 2H, −NH$_2$), 4.51 (s, 2H, −CH$_2$-). ^{13}C NMR (100 MHz, DMSO-d_6, δ, ppm) δ 181.55, 139.78, 128.06, 127.31, 126.62, 46.12. HR-MS (ESI), calcd. C$_8$H$_{11}$N$_3$S, [M+Na]$^+$$m/z$: 204.0572. found: 204.0573.

4.3.3. N-phenethylhydrazinecarbothioamide(**3c**)

White solid, yield 85%. ^{1}H NMR (400 MHz, DMSO-d_6, δ, ppm) δ 8.64 (s, 1H, −NH−), 7.87 (s, 1H, −NH−), 7.41−7.13 (m, 5H, Ar−H), 4.43 (s, 2H, −NH$_2$), 3.67 (dd, J = 14.7, 6.2 Hz, 2H, −CH$_2$-), 2.92−2.75 (m, 2H, −CH$_2$-). ^{13}C NMR (100 MHz, DMSO-d_6, δ, ppm) δ 181.13, 139.40, 128.56, 128.35, 126.06, 44.37, 35.17. HR-MS (ESI), calcd. C$_9$H$_{13}$N$_3$S, [M+H]$^+$$m/z$: 196.0908. found: 196.0905.

4.3.4. N-(2-morpholinoethyl) hydrazinecarbothioamide(**3d**)

White solid, yield 78%. ^{1}H NMR (400 MHz, DMSO-d_6, δ, ppm) δ 8.63 (s, 1H, −NH−), 7.83 (s, 1H, −NH−), 4.45 (s, 2H, −NH$_2$), 3.56 (dd, J = 8.6, 4.5 Hz, 6H, −CH$_2$-), 2.44 (t, J = 6.5 Hz, 2H, −CH$_2$-), 2.39 (s, 4H, −CH$_2$-). ^{13}C NMR (100 MHz, DMSO-d_6, δ, ppm) δ 181.05, 66.19, 56.99, 53.18. HR-MS (ESI), calcd. C$_7$H$_{16}$N$_4$OS, [M+H]$^+$$m/z$: 205.1123. found: 205.1122.

4.3.5. N-(2-(1H-indol-3-yl) ethyl) hydrazinecarbothioamide(**3e**)

White solid, yield 74%. ^{1}H NMR (400 MHz, DMSO-d_6, δ, ppm) δ 10.81 (s, 1H, −NH−), 8.62 (s, 1H, −NH−), 7.94 (s, 1H, −NH−), 7.68 (d, J = 7.8 Hz, 1H, Ar−H), 7.34 (d, J = 8.1 Hz, 1H, Ar−H), 7.17 (d, J = 1.9 Hz, 1H, Ar−H), 7.07 (t, J = 7.2 Hz, 1H, Ar−H), 6.98 (t, J = 7.4 Hz, 1H, Ar−H), 4.43 (s, 2H, −NH$_2$), 3.75 (dd, J = 13.9, 6.8 Hz, 2H, −CH$_2$-), 2.93 (t, J = 7.5 Hz, 2H, −CH$_2$-). ^{13}C NMR (100 MHz, DMSO-d_6, δ, ppm) δ 181.57, 136.77, 127.73, 123.06, 121.43, 119.07, 118.68, 112.23, 111.80, 44.06, 25.77. HR-MS (ESI), calcd. C$_{11}$H$_{14}$N$_4$S, [M+Na] $^+$$m/z$: 257.0837. found: 257.0836.

4.3.6. tert-butyl 4-(2-(hydrazinecarbothioamido) ethyl) piperazine-1-carboxylate(**3f**)

White solid, yield 74%. ^{1}H NMR (400 MHz, DMSO-d_6, δ, ppm) δ 8.63 (s, 1H, −NH−), 7.83 (s, 1H, −NH−), 4.44 (s, 2H, −NH$_2$), 3.55 (dd, J = 12.0, 6.1 Hz, 2H, −CH$_2$-), 3.30 (s, 2H, −CH$_2$-), 2.46 (t, J = 6.5 Hz, 2H, −CH$_2$-), 2.41−2.29 (m, 4H, −CH$_2$-), 1.39 (s, 9H, −CH$_3$). ^{13}C NMR (100 MHz, DMSO-d_6, δ, ppm) δ 181.14, 153.79, 78.71, 56.51, 52.39, 28.03. HR-MS (ESI), calcd. C$_{12}$H$_{25}$N$_5$O$_2$S, [M+H]$^+$$m/z$: 304.1807. found: 304.1807.
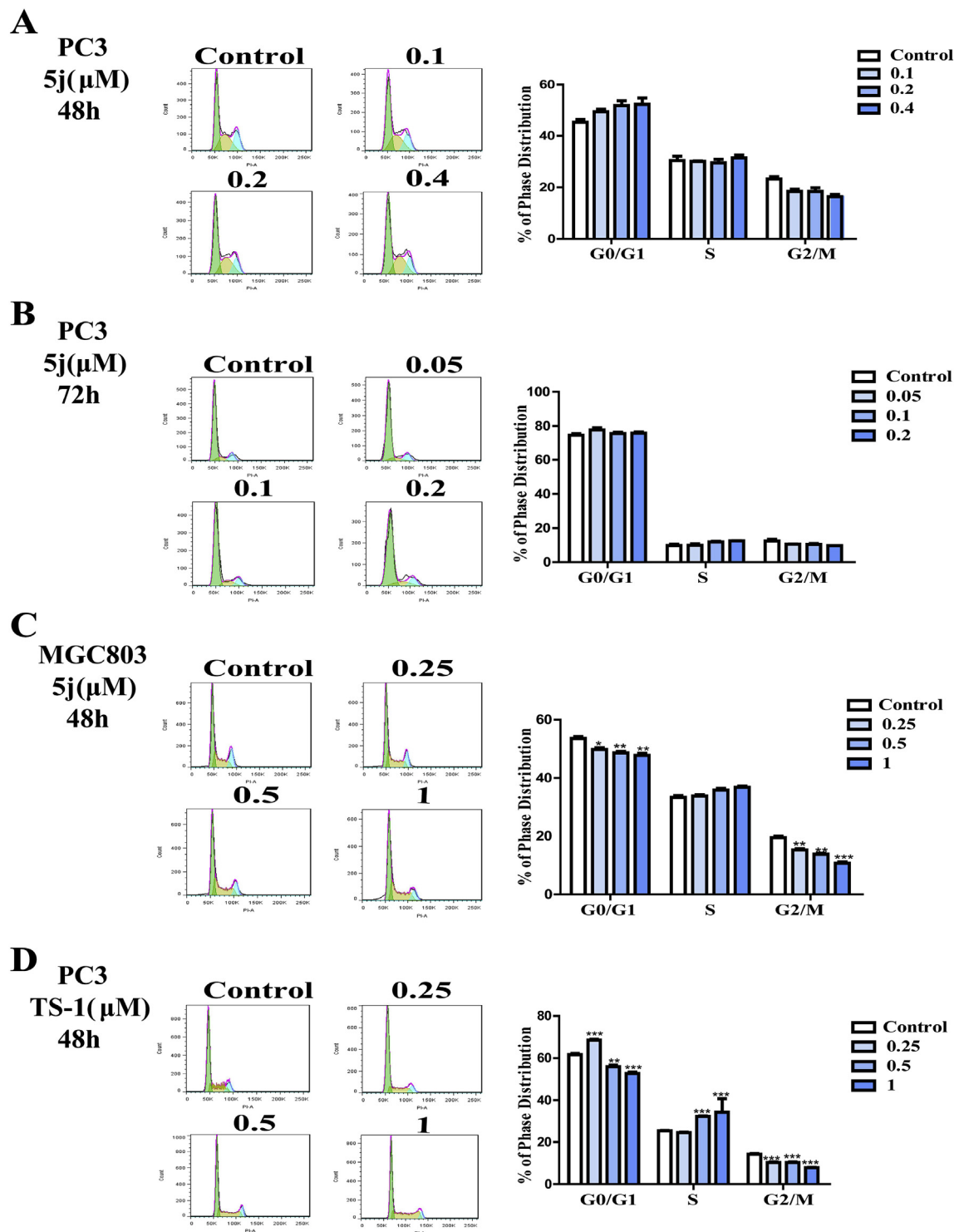
Fig. 7. Effect of compound **5j** and **TS-1** on cell cycle. (A) Cell cycle analysis of PC3 cells treatment of compound **5j** for 48 h (B) Cell cycle analysis of PC3 cells treatment of compound **5j** for 72 h (C) Cell cycle analysis of MGC803 cells treatment of compound **5j** for 48 h (D) Cell cycle analysis of PC3 cells treatment of compound **TS-1** for 48 h. The dates were represented as the Mean ± SD. All experiments were performed at least three times. $^{*}p < 0.5$, $^{**}p < 0.01$, $^{***}p < 0.001$ compared with the control.

4.3.7. N-(2-(5-methyl-1H-indol-3-yl) ethyl) hydrazinecarbothioamide(3g)

White solid, yield 75%. ^{1}H NMR (400 MHz, DMSO-d_6, δ, ppm) δ 10.67 (s, 1H, −NH−), 8.62 (s, 1H, −NH−), 7.92 (s, 1H, Ar−H), 7.44 (s, 1H, Ar−H), 7.22 (d, $J = 8.2$ Hz, 1H, −NH−), 7.10 (s, 1H, Ar−H), 6.89 (d, $J = 8.2$ Hz, 1H, Ar−H), 4.43 (s, 2H, −NH$_2$), 3.72 (dd, $J = 13.8$, 6.7 Hz, 2H, −CH$_2$-), 2.89 (t, $J = 7.5$ Hz, 2H, −CH$_2$-), 2.38 (s, 3H, −CH$_3$). ^{13}C NMR (100 MHz, DMSO-d_6, δ, ppm) δ 181.03, 134.64, 127.43, 126.51, 122.64, 122.53, 118.16, 111.16, 111.01, 43.53, 25.25, 21.29. HR-MS (ESI), calcd. C$_{12}$H$_{16}$N$_4$S, [M+H] $^{+}m/z$: 249.1174. found: 249.1174.

4.3.8. N-(2-(5-methoxy-1H-indol-3-yl) ethyl) hydrazinecarbothioamide(3h)

White solid, yield 72%. ^{1}H NMR (400 MHz, DMSO-d_6, δ, ppm)

δ 10.65 (s, 1H, −NH−), 8.65 (s, 1H, −NH−), 7.98 (s, 1H, Ar−H), 7.24 (s, 1H, Ar−H), 7.21 (d, $J = 8.8$ Hz, 1H, −NH−), 7.11 (s, 1H, Ar−H), 6.71 (dd, $J = 8.7, 2.1$ Hz, 1H, Ar−H), 4.44 (s, 2H, −NH$_2$), 3.76 (s, 3H, −CH$_3$), 3.70 (d, $J = 6.6$ Hz, 2H, −CH$_2$-), 2.88 (t, $J = 7.6$ Hz, 2H, −CH$_2$-). ^{13}C NMR (100 MHz, DMSO-d_6, δ, ppm) δ 181.05, 152.89, 131.37, 127.57, 123.18, 111.90, 111.45, 111.09, 100.49, 55.30, 43.44, 25.41. HR-MS (ESI), calcd. C$_{12}$H$_{16}$N$_4$OS, [M+H] $^+ m/z$: 265.1123. found: 265.1125.

4.3.9. N-(2-(5-chloro-1H-indol-3-yl) ethyl) hydrazinecarbothioamide(3i)

White solid, yield 69%. ^{1}H NMR (400 MHz, DMSO-d_6, δ, ppm) δ 11.04 (s, 1H, −NH−), 8.66 (s, 1H, −NH−), 8.01 (s, 1H, Ar−H), 7.76 (s, 1H, Ar−H), 7.35 (d, $J = 8.6$ Hz, 1H, −NH−), 7.25 (s, 1H, Ar−H), 7.15−7.00 (m, 1H, Ar−H), 4.45 (s, 2H, −NH$_2$), 3.70 (dd, $J = 14.0$, 6.6 Hz, 2H, −CH$_2$-), 2.90 (t, $J = 7.6$ Hz, 2H, −CH$_2$-). ^{13}C NMR (100 MHz, DMSO-d_6, δ, ppm) δ 181.01, 134.69, 128.41, 124.52, 122.92, 120.85, 117.93, 112.82, 111.73, 105.18, 43.49, 29.57, 25.14, 0.73. HR-MS (ESI), calcd. C$_{11}$H$_{13}$ClN$_4$S, [M+H]$^+ m/z$: 269.0628. found: 269.0626.

4.3.10. N-(2-(5-bromo-1H-indol-3-yl) ethyl) hydrazinecarbothioamide(3j)

White solid, yield 71%. 1H NMR (400 MHz, DMSO-d_6, δ, ppm) δ 11.05 (s, 1H, −NH−), 8.65 (s, 1H, −NH−), 7.96 (d, $J = 38.6$ Hz, 2H, Ar−H), 7.49−7.06 (m, 3H, −NH−, 2Ar−H), 4.44 (s, 2H, −NH$_2$), 3.70 (dd, $J = 13.5, 6.5$ Hz, 2H, −CH$_2$-), 2.90 (t, $J = 7.5$ Hz, 2H, −CH$_2$-). ^{13}C NMR (100 MHz, DMSO-d_6, δ, ppm) δ 181.01, 134.92, 129.13, 124.36, 123.36, 120.97, 113.31, 111.66, 110.91, 43.52, 25.13. HR-MS (ESI), calcd. C$_{11}$H$_{13}$BrN$_4$S, [M+Na]$^+ m/z$: 334.9942. found: 334.9944.

4.3.11. N-(2-(2-methyl-1H-indol-3-yl) ethyl) hydrazinecarbothioamide(3k)

White solid, yield 65%. ^{1}H NMR (400 MHz, DMSO-d_6, δ, ppm) δ 10.72 (s, 1H, −NH−), 8.64 (s, 1H, −NH−), 7.92 (s, 1H, Ar−H), 7.56 (d, $J = 7.6$ Hz, 1H, Ar−H), 7.22 (d, $J = 7.8$ Hz, 1H, −NH−), 6.94 (dt, $J = 14.5, 7.0$ Hz, 2H, Ar−H), 4.43 (s, 2H, −NH$_2$), 3.58 (dd, $J = 14.3$, 6.5 Hz, 2H, −CH$_2$-), 2.94−2.75 (m, 2H, −CH$_2$-), 2.35 (s, 3H, −CH$_3$). ^{13}C NMR (100 MHz, DMSO-d_6, δ, ppm) δ 181.03, 135.19, 132.14, 128.29, 119.89, 118.01, 117.59, 110.26, 107.39, 43.67, 24.10, 11.20. HR-MS (ESI), calcd. C$_{12}$H$_{16}$N$_4$S, [M+Na]$^+ m/z$: 271.0993. found: 271.0996.

4.4. General procedure for the synthesis of compounds(4a-f,5a-v)

To the solution of **3a-k** (0.64 mmol) in ethanol containing acetic acid (0.064 mmol), appropriate aldehyde or ketone (0.77 mmol) was added. The mixture was kept at room temperature for 2 h, the formed precipitation was filtered, and the left residue was washed with ethanol to give compounds **4a-f** and **5a-v** as solid in 45−85% yield.

4.4.1. (E)-N-phenyl-2-(pyridin-2-ylmethylene) hydrazine-1-carbothioamide(4a)

White solid, m. p. 198.7−199.8 °C, yield 70%. ^{1}H NMR (400 MHz, DMSO-d_6, δ, ppm) δ 12.03 (s, 1H, −NH−), 10.25 (s, 1H, −NH−), 8.64−8.53 (m, 1H, Ar−H), 8.45 (d, $J = 8.0$ Hz, 1H, Ar−H), 8.21 (s, 1H, −CH=N−), 7.88−7.76 (m, 1H, Ar−H), 7.56 (d, $J = 7.6$ Hz, 2H, Ar−H), 7.45−7.33 (m, 3H, Ar−H), 7.23 (s, $J = 7.4$ Hz, 1H, Ar−H). ^{13}C NMR (100 MHz, DMSO-d_6, δ, ppm) δ 176.41, 153.16, 149.32, 143.06, 138.93, 136.45, 128.08, 126.06, 125.51, 124.21, 120.58. HR-MS (ESI), calcd. C$_{13}$H$_{12}$N$_4$S, [M+H]$^+ m/z$: 257.0861. found: 257.0862.

4.4.2. (E)-N-benzyl-2-(pyridin-2-ylmethylene) hydrazine-1-carbothioamide(4b)

Yellow solid, m. p. 180.6−190.5 °C, yield 66%. ^{1}H NMR (400 MHz, DMSO-d_6, δ, ppm) δ 11.82 (s, 1H, −NH−), 9.25 (t, $J = 6.1$ Hz, 1H, −NH−), 8.57 (d, $J = 4.3$ Hz, 1H, Ar−H), 8.29 (d, $J = 8.0$ Hz, 1H, Ar−H), 8.14 (s, 1H, −CH=N-), 7.87−7.79 (m, 1H, −NH−), 7.42−7.17 (m, 6H, Ar−H), 4.85 (t, $J = 9.4$ Hz, 2H, −CH$_2$-). ^{13}C NMR (100 MHz, DMSO-d_6, δ, ppm) δ 177.86, 153.29, 149.32, 142.48, 139.24, 136.41, 128.15, 127.18, 126.72, 124.06, 120.20, 46.62. HR-MS (ESI), calcd. C$_{14}$H$_{14}$N$_4$S, [M+H]$^+ m/z$: 271.1017. found: 271.1017.

4.4.3. (E)-N-phenethyl-2-(pyridin-2-ylmethylene) hydrazine-1-carbothioamide(4c)

Yellow solid, m. p. 175.6−177.1 °C, yield 65%. ^{1}H NMR (400 MHz, DMSO-d_6, δ, ppm) δ 11.74 (s, 1H, −NH−), 8.73 (t, $J = 5.8$ Hz, 1H, −NH−), 8.57 (d, $J = 4.3$ Hz, 1H, Ar−H), 8.20 (d, $J = 8.0$ Hz, 1H, Ar−H), 8.10 (s, 1H, −CH=N−), 7.86 (td, $J = 7.7, 1.4$ Hz, 1H, Ar−H), 7.44−7.15 (m, 6H, Ar−H), 3.86−3.61 (m, 2H, −CH$_2$-), 3.01−2.85 (m, 2H, −CH$_2$-). ^{13}C NMR (100 MHz, DMSO-d_6, δ, ppm) δ 177.20, 153.28, 149.35, 142.16, 139.15, 136.45, 128.57, 128.44, 126.19, 124.05, 120.02, 45.07, 34.77. HR-MS (ESI), calcd. C$_{15}$H$_{16}$N$_4$S, [M+H]$^+ m/z$: 285.1174. found: 285.1175.

4.4.4. (E)-N-(2-morpholinoethyl)-2-(pyridin-2-ylmethylene) hydrazine-1-carbothioamide(4d)

White solid, m. p. 165.3−166.0 °C, yield 45%. ^{1}H NMR (400 MHz, DMSO-d_6, δ, ppm) δ 11.74 (s, 1H, −NH−), 8.67−8.47 (m, 2H, −NH−, Ar−H), 8.17 (d, $J = 8.0$ Hz, 1H, Ar−H), 8.10 (s, 1H, −CH=N−), 7.86 (td, $J = 7.8, 1.3$ Hz, 1H, Ar−H), 7.42−7.34 (m, 1H, Ar−H), 3.69 (dd, $J = 12.6, 6.4$ Hz, 2H, −CH$_2$-), 3.64−3.51 (m, 4H, −CH$_2$-), 2.55 (t, $J = 6.3$ Hz, 2H, −CH$_2$-), 2.45 (s, 4H, −CH$_2$-). ^{13}C NMR (100 MHz, DMSO-d_6, δ, ppm) δ 177.17, 153.23, 149.41, 142.14, 136.49, 124.10, 119.82, 66.26, 56.50, 53.21. HR-MS (ESI), calcd. C$_{13}$H$_{19}$N$_5$OS, [M+H]$^+ m/z$: 294.1388. found: 294.1387.

4.4.5. (E)-N-(2-(1H-indol-3-yl)ethyl)-2-(pyridin-2-ylmethylene) hydrazine-1-carbothioamide(4e)

Yellow solid, m. p. 191.0−193.2 °C, yield 68%. ^{1}H NMR (400 MHz, DMSO-d_6, ppm) δ 11.73 (s, 1H, −NH−), 10.86 (s, 1H, −NH−), 8.74 (t, $J = 5.5$ Hz, 1H, −NH−), 8.57 (s, $J = 4.4$ Hz, 1H, Ar−H), 8.14 (d, $J = 8.0$ Hz, 1H, Ar−H), 8.11 (s, 1H, Ar−H), 7.87 (d, $J = 7.4$ Hz, 1H, Ar−H), 7.73 (d, $J = 7.8$ Hz, 1H, Ar−H), 7.37 (dd, $J = 11.9, 7.4$ Hz, 2H, Ar−H), 7.22 (s, 1H, −CH=N−), 7.08 (t, $J = 7.4$ Hz, 1H, Ar−H), 6.99 (t, $J = 7.4$ Hz, 1H, Ar−H), 3.86 (dd, $J = 11.4, 6.5$ Hz, 2H, −CH$_2$-), 3.04 (d, $J = 7.4$ Hz, 2H, −CH$_2$-). ^{13}C NMR (100 MHz, DMSO-d_6, δ, ppm) δ 177.57, 153.75, 149.82, 142.57, 136.97, 127.73, 124.51, 123.13, 121.46, 120.48, 119.03, 118.73, 111.85, 44.89, 25.30. HR-MS (ESI), calcd. C$_{17}$H$_{17}$N$_5$S, [M+H]$^+ m/z$: 324.1283. found: 324.1284.

4.4.6. tert-butyl(E)-4-(2-(2-(pyridin-2-ylmethylene) hydrazine-1-carbothioamido) ethyl) piperazine-1-carboxylate(4f)

Yellow solid, m. p. 155.8−158.2 °C, yield 55%. ^{1}H NMR (400 MHz, DMSO-d_6, δ, ppm) δ 11.73 (s, 1H, −NH−), 8.66−8.51 (m, 2H, −NH−, Ar−H), 8.17 (d, $J = 8.0$ Hz, 1H, Ar−H), 8.10 (s, 1H, −CH=N-), 7.90−7.78 (m, 1H, Ar−H), 7.38 (dd, $J = 6.9, 5.4$ Hz, 1H, Ar−H), 3.69 (dd, $J = 12.8, 6.4$ Hz, 2H, −CH$_2$-), 3.32 (s, 4H, −CH$_2$-), 2.57 (d, $J = 6.9$ Hz, 2H, −CH$_2$-), 2.46−2.36 (m, 4H, −CH$_2$-), 1.40 (s, 9H, −CH$_3$). ^{13}C NMR (100 MHz, DMSO-d_6, δ, ppm) δ 177.19, 153.80, 153.24, 149.40, 142.14, 136.45, 124.08, 119.88, 78.72, 56.08, 52.44, 40.67, 28.04. HR-MS (ESI), calcd. C$_{18}$H$_{28}$N$_6$O$_2$S, [M+H]$^+ m/z$: 393.2072. found: 393.2071.

4.4.7. (E)-N-(2-(5-methyl-1H-indol-3-yl)ethyl)-2-(pyridin-2-ylmethylene)hydrazine-1-carbothioamide(5a)

White solid, m. p. 177.2−179.0 °C, yield 58%. ^{1}H NMR (400 MHz, DMSO-d_6, ppm) δ 11.75 (s, 1H, −NH−), 10.73 (s, 1H, −NH−), 8.81−8.66 (m, 1H, −NH−), 8.57 (s, $J = 4.8$ Hz, 1H, Ar−H), 8.13 (s, 1H, Ar−H), 8.11 (s, 1H, Ar−H), 7.96−7.75 (m, 1H, Ar−H), 7.46 (d,

J = 13.8 Hz, 1H, Ar−H), 7.38 (dd, *J* = 6.8, 5.4 Hz, 1H, Ar−H), 7.23 (s, *J* = 7.5 Hz, 1H, −CH=N-), 7.15 (dd, *J* = 17.2, 6.3 Hz, 1H, Ar−H), 6.90 (d, *J* = 8.2 Hz, 1H, Ar−H), 3.82 (dt, *J* = 37.6, 18.8 Hz, 2H, −CH$_2$-), 3.11−2.82 (m, 2H, −CH$_2$-), 2.36 (s, 3H, −CH$_3$). ^{13}C NMR (100 MHz, DMSO-d_6, δ, ppm) δ 177.06, 153.27, 149.33, 142.06, 136.47, 134.66, 127.48, 126.60, 124.02, 122.75, 122.59, 119.97, 118.12, 111.06, 111.00, 44.42, 24.78, 21.28. HR-MS (ESI), calcd. C$_{18}$H$_{19}$N$_5$S, [M+H]$^+$ *m/z*: 338.1439. found: 338.1441.

4.4.8. (E)-N-(2-(5-methoxy-1H-indol-3-yl)ethyl)-2-(pyridin-2-ylmethylene)hydrazine-1-carbothioamide(5b)

White solid, m. p. 118.2−120.4 °C, yield 68%. ^{1}H NMR (400 MHz, DMSO-d_6, ppm) δ 11.75 (s, 1H, −NH−), 10.70 (s, 1H, −NH−), 8.75 (t, *J* = 5.7 Hz, 1H, −NH−), 8.59 (s, *J* = 13.5 Hz, 1H, Ar−H), 8.14 (d, *J* = 8.0 Hz, 1H, Ar−H), 8.11 (s, 1H, Ar−H), 7.92−7.77 (m, 1H, Ar−H), 7.39 (dd, *J* = 11.2, 5.9 Hz, 1H, Ar−H), 7.26 (dd, *J* = 8.3, 5.4 Hz, 2H, Ar−H), 7.16 (s, *J* = 12.2 Hz, 1H, −CH=N-), 6.73 (dd, *J* = 8.7, 2.1 Hz, 1H, Ar−H), 3.85 (dd, *J* = 14.4, 6.5 Hz, 2H, −CH$_2$-), 3.76 (s, 3H, −CH$_3$), 3.09−2.89 (m, 2H, −CH$_2$-). ^{13}C NMR (100 MHz, DMSO-d_6, δ, ppm) δ 177.09, 153.26, 152.96, 149.33, 142.09, 136.48, 131.39, 127.61, 124.03, 123.29, 119.99, 111.98, 111.26, 111.13, 55.28, 44.30, 24.89. HR-MS(ESI), calcd. C$_{18}$H$_{19}$N$_5$OS, [M+Na]$^+$ *m/z*: 376.1208. found: 376.1209.

4.4.9. (E)-N-(2-(5-chloro-1H-indol-3-yl)ethyl)-2-(pyridin-2-ylmethylene)hydrazine-1-carbothioamide(5c)

White solid, m. p. 183.6−185.2 °C, yield 71%. ^{1}H NMR (400 MHz, DMSO-d_6, ppm) δ 11.76 (s, 1H, −NH−),11.08 (s, 1H, −NH−), 8.78 (t, 1H, −NH−), 8.56 (s, 1H, Ar−H), 8.15 (d, *J* = 7.4 Hz, 1H, Ar−H), 8.11 (s, 1H, Ar−H), 7.85 (s, 1H, Ar−H), 7.77 (s, 1H, Ar−H), 7.36 (d, *J* = 8.0 Hz, 2H, Ar−H), 7.30 (s, 1H, −CH=N-), 7.06 (d, *J* = 7.6 Hz, 1H, Ar−H), 3.81 (s, 2H, −CH$_2$-), 3.01 (s, 2H, −CH$_2$-). ^{13}C NMR (100 MHz, DMSO-d_6, δ, ppm) δ 177.09, 153.28, 149.33, 142.16, 136.46, 134.70, 128.45, 124.65, 124.03, 123.02, 120.90, 120.00, 117.86, 112.89, 111.53, 44.36, 24.63. HR-MS(ESI), calcd. C$_{17}$H$_{16}$ClN$_5$S, [M+Na]+*m/z*: 380.0713. found: 380.0710.

4.4.10. (E)-N-(2-(5-bromo-1H-indol-3-yl)ethyl)-2-(pyridin-2-ylmethylene)hydrazine-1-carbothioamide(5d)

White solid, m. p. 182.6−184.2 °C, yield 65%. ^{1}H NMR (400 MHz, DMSO-d_6, ppm) δ 11.77 (s, 1H, −NH−), 11.10 (s, 1H, −NH−), 8.78 (t, *J* = 5.7 Hz, 1H, −NH−), 8.58 (s, *J* = 4.6 Hz, 1H, Ar−H), 8.15 (s, *J* = 8.0 Hz, 1H, Ar−H), 8.12 (s, 1H, Ar−H), 7.92 (s, 1H, Ar−H), 7.86 (t, *J* = 7.7 Hz, 1H, Ar−H), 7.40 (dd, *J* = 12.7, 6.8 Hz, 1H, Ar−H), 7.33 (d, *J* = 8.6 Hz, 1H, −NH−), 7.30 (s, 1H, −CH=N-), 7.18 (d, *J* = 8.6 Hz, 1H, Ar−H), 3.82 (dd, *J* = 14.4, 6.6 Hz, 2H, −CH$_2$-), 3.23−2.80 (m, 2H, −CH$_2$-). ^{13}C NMR (100 MHz, DMSO-d_6, δ, ppm) δ 177.09, 153.28, 149.33, 142.17, 136.46, 134.93, 129.17, 124.48, 124.03, 123.42, 120.89, 120.01, 113.37, 111.46, 111.00, 44.37, 24.63. HR-MS (ESI), calcd. C$_{17}$H$_{16}$BrN$_5$S, [M+Na]$^+$ *m/z*: 424.0207. found: 424.0209.

4.4.11. (E)-N-(2-(2-methyl-1H-indol-3-yl)ethyl)-2-(pyridin-2-ylmethylene)hydrazine-1-carbothioamide(5e)

Yellow solid, m. p. 108.2−109.5 °C, yield 80%. ^{1}H NMR (400 MHz, DMSO-d_6, ppm) δ 11.75 (s, 1H-, −NH−), 10.77 (s, 1H-, −NH−), 8.76 (d, *J* = 22.3 Hz, 1H, −NH−), 8.58 (s, *J* = 3.6 Hz, 1H, Ar−H), 8.13 (d, *J* = 8.1 Hz, 1H, Ar−H), 8.11 (s, 1H, Ar−H), 7.93−7.76 (m, 1H, Ar−H), 7.61 (t, *J* = 13.5 Hz, 1H, Ar−H), 7.40 (d, *J* = 5.1 Hz, 1H, −NH−), 7.25 (s, *J* = 7.5 Hz, 1H, −CH=N-), 6.96 (dt, *J* = 20.1, 7.1 Hz, 2H, Ar−H), 3.71 (d, *J* = 6.2 Hz, 2H, −CH$_2$-), 3.05−2.87 (m, 3H, −CH$_2$-), 2.39 (s, 3H, −CH$_3$). ^{13}C NMR (100 MHz, DMSO-d_6, δ, ppm) δ 177.09, 153.26, 149.35, 142.03, 136.47, 135.20, 132.20, 128.37, 124.04, 119.96, 118.10, 117.53, 110.34, 107.18, 48.57, 44.38, 23.61, 11.23. HR-MS(ESI), calcd. C$_{18}$H$_{19}$N$_5$S, [M+Na]$^+$*m/z*: 360.1259. found: 360.1260.

4.4.12. (E)-N-(2-(1H-indol-3-yl)ethyl)-2-((5-methoxypyridin-2-yl)methylene)hydrazine-1-carbothioamide(5f)

Yellow solid, m. p. 226.5−228.2 °C, yield 67%. ^{1}H NMR (400 MHz, DMSO-d_6, ppm) δ 11.61 (s, 1H, −NH−), 11.07 (s, 1H, −NH−), 8.67 (dd, *J* = 15.1, 9.3 Hz, 1H, NH-), 8.29 (s, *J* = 2.8 Hz, 1H, Ar−H), 8.10 (d, *J* = 8.9 Hz, 1H, Ar−H), 8.09 (s, 1H, Ar−H), 7.78 (d, *J* = 1.8 Hz, 1H, Ar−H), 7.47 (dd, *J* = 8.8, 2.8 Hz, 1H, Ar−H), 7.37 (d, *J* = 8.6 Hz, 1H, −CH=N-), 7.31 (d, *J* = 2.0 Hz, 1H, Ar−H), 7.07 (dd, *J* = 8.6, 1.9 Hz, 1H, Ar−H), 4.00−3.87 (m, 3H, −CH$_3$), 3.79 (dt, *J* = 38.6, 19.3 Hz, 2H, −CH$_2$-), 2.99 (dd, *J* = 25.9, 18.4 Hz, 2H, −CH$_2$-). ^{13}C NMR (100 MHz, DMSO-d_6, δ, ppm) δ 176.91, 155.84, 145.82, 142.14, 136.56, 134.72, 128.45, 124.63, 123.02, 121.33, 120.94, 120.91, 117.87, 112.89, 111.58, 55.79, 44.27, 24.70. HR-MS (ESI), calcd. C$_{18}$H$_{19}$N$_5$OS, [M+H]$^+$*m/z*: 388.09. found:388.09.

4.4.13. (E)-N-(2-(1H-indol-3-yl)ethyl)-2-((5-hydroxypyridin-2-yl)methylene)hydrazine-1-carbothioamide(5g)

Yellow solid, m. p. 215.2−218.5 °C, yield 78%. ^{1}H NMR (400 MHz, DMSO-d_6, ppm) δ 11.56 (s, 1H, −NH−), 11.06 (d, *J* = 14.7 Hz, 1H, −NH−), 10.35 (s, 1H, −OH), 8.60 (t, *J* = 5.7 Hz, 1H, −NH−), 8.11 (t, *J* = 8.9 Hz, 1H, Ar−H), 8.05 (s, 1H, Ar−H), 7.98 (d, *J* = 8.7 Hz, 1H, Ar−H), 7.77 (t, *J* = 4.6 Hz, 1H, Ar−H), 7.37 (d, *J* = 8.6 Hz, 1H, Ar−H), 7.30 (s, *J* = 5.9 Hz, 1H, −CH=N-), 7.23 (dd, *J* = 8.7, 2.6 Hz, 1H, Ar−H), 7.07 (dd, *J* = 8.6, 1.9 Hz, 1H, Ar−H), 3.79 (dt, *J* = 32.0, 15.9 Hz, 2H, −CH$_2$-), 3.14−2.83 (m, 2H, −CH$_2$-). ^{13}C NMR (100 MHz, DMSO-d_6, δ, ppm) δ 176.83, 154.39, 144.39, 142.57, 137.32, 134.71, 128.46, 124.64, 123.03, 122.71, 121.13, 120.90, 117.86, 112.88, 111.58, 44.26, 24.69. HR-MS (ESI), calcd. C$_{17}$H$_{17}$N$_5$OS, [M+H]$^+$*m/z*: 374.08. found:374.08.

4.4.14. (E)-N-(2-(5-chloro-1H-indol-3-yl)ethyl)-2-((5-chloropyridin-2-yl)methylene)hydrazine-1-carbothioamide(5h)

White solid, m. p. 236.5−236.6 °C, yield 69%. ^{1}H NMR (400 MHz, DMSO-d_6, ppm) δ 11.80 (s, 1H, −NH−), 11.07 (s, 1H, −NH−), 8.84 (t, *J* = 5.8 Hz, 1H, −NH−), 8.62 (s, *J* = 2.3 Hz, 1H, Ar−H), 8.21 (d, *J* = 8.6 Hz, 1H, Ar−H), 8.07 (s, *J* = 18.3 Hz, 1H, Ar−H), 8.01 (dd, *J* = 8.6, 2.4 Hz, 1H, Ar−H), 7.76 (d, *J* = 1.8 Hz, 1H, Ar−H), 7.37 (d, *J* = 8.6 Hz, 1H, Ar−H), 7.31 (s, *J* = 2.1 Hz, 1H, −CH=N-), 7.07 (dd, *J* = 8.6, 2.0 Hz, 1H, Ar−H), 3.82 (dd, *J* = 14.9, 6.3 Hz, 2H, −CH$_2$-), 3.08−2.88 (m, 2H, −CH$_2$-). ^{13}C NMR (100 MHz, DMSO-d_6, δ, ppm) δ 177.17, 151.95, 147.84, 140.80, 136.38, 134.73, 131.11, 128.46, 124.64, 123.03, 121.19, 120.90, 117.84, 112.89, 111.54, 44.39, 24.60. HR-MS (ESI), calcd. C$_{17}$H$_{15}$Cl$_2$N$_5$S, [M+ Na]$^+$*m/z*: 414.0323. found: 414.0322.

4.4.15. (E)-2-((5-bromopyridin-2-yl)methylene)-N-(2-(5-chloro-1H-indol-3-yl)ethyl)hydrazine-1-carbothioamide(5i)

White solid, m. p. 232.6−233.5 °C, yield 61%. ^{1}H NMR (400 MHz, DMSO-d_6, ppm) δ 11.80 (s, 1H, −NH−), 11.04 (d, *J* = 17.2 Hz, 1H, −NH−), 8.84 (t, *J* = 5.8 Hz, 1H, −NH−), 8.70 (s, 1H, Ar−H), 8.23−8.11 (m, 2H, Ar−H), 8.08 (s, 1H, Ar−H), 7.76 (d, *J* = 1.6 Hz, 1H, Ar−H), 7.36 (t, *J* = 8.0 Hz, 1H, Ar−H), 7.29 (t, *J* = 11.1 Hz, 1H, −CH=N-), 7.07 (dd, *J* = 8.6, 1.9 Hz, 1H, Ar−H), 3.82 (dd, *J* = 14.7, 6.5 Hz, 2H, −CH$_2$-), 3.00 (dd, *J* = 25.5, 18.1 Hz, 2H, −CH$_2$-). ^{13}C NMR (100 MHz, DMSO-d_6, δ, ppm) δ 177.13, 152.17, 150.02, 140.89, 139.13, 134.72, 128.44, 124.65, 123.02, 121.58, 120.90, 120.42, 117.85, 44.37, 24.61. HR-MS (ESI),-calcd. C$_{28}$H$_{28}$BrClN$_6$OS, [M+Na]$^+$*m/z*: 457.9818.found: 457.9817.

4.4.16. (E)-N-(2-(5-chloro-1H-indol-3-yl)ethyl)-2-((5-methylpyridin-2-yl)methylene)hydrazine-1-carbothioamide(5j)

White solid, m. p. 225.6−227.1 °C, yield 67%. ^{1}H NMR (400 MHz, DMSO-d_6, ppm) δ 11.71 (s, 1H, −NH−), 11.09 (s, 1H, −NH−), 8.74 (d, *J* = 5.5 Hz, 1H, −NH−), 8.41 (s, 1H, Ar−H), 8.08 (s, 1H, Ar−H), 8.06 (d, *J* = 8.2 Hz, 1H, Ar−H), 7.78 (s, 1H, Ar−H), 7.68 (d, *J* = 8.0 Hz, 1H, Ar−H), 7.37 (d, *J* = 8.5 Hz, 1H, Ar−H), 7.25 (s, 1H, −CH=N-), 7.07 (d, *J* = 8.4 Hz, 1H, Ar−H), 3.81 (d, *J* = 7.0 Hz, 2H, −CH$_2$-), 3.07−2.84 (m, 2H, −CH$_2$-), 2.32 (s, 3H, -CH3). ^{13}C NMR (100 MHz, DMSO-d_6, δ,

ppm) δ 176.99, 150.70, 149.53, 142.31, 136.89, 134.70, 133.70, 128.45, 124.63, 123.01, 120.90, 119.53, 117.87, 112.89, 111.55, 44.32, 24.67, 17.90. HR-MS (ESI), calcd. $C_{18}H_{18}ClN_5S$, [M+H]$^+$ m/z: 372.1050. found: 372.1051.

4.4.17. (E)-N-(2-(5-chloro-1H-indol-3-yl)ethyl)-2-((3-methylpyridin-2-yl)methylene)hydrazine-1-carbothioamide(5k)

White solid, m. p. 219.2−219.5 °C, yield 55%. ^{1}H NMR (400 MHz, DMSO-d_6, ppm) δ 11.69 (s, 1H, −NH−), 11.06 (s, 1H, −NH−), 8.46 (d, J = 4.2 Hz, 1H, −NH−), 8.32 (s, 1H, Ar−H), 8.02 (t, J = 5.7 Hz, 1H, Ar−H), 7.73 (s, J = 4.1 Hz, 1H, −CH=N−), 7.65 (d, J = 7.6 Hz, 1H, Ar−H), 7.36 (d, J = 8.6 Hz, 1H, Ar−H), 7.28 (t, J = 6.1 Hz, 2H, Ar−H), 7.05 (dd, J = 8.6, 1.8 Hz, 1H, Ar−H), 3.86 (dd, J = 13.4, 6.8 Hz, 2H, −CH$_2$-), 2.96 (d t, J = 39.6, 7.4 Hz, 2H, −CH$_2$-), 2.37 (s, 3H, −CH$_3$). ^{13}C NMR (100 MHz, DMSO-d_6, δ, ppm) δ 175.93, 140.22, 134.84, 131.62, 128.43, 124.60, 123.03, 120.95, 120.58, 117.97, 112.90, 111.60, 111.24, 108.93, 108.70, 98.06, 97.81, 48.57, 43.82, 24.90. HR-MS (ESI), calcd. $C_{18}H_{18}ClN_5S$, [M+H]$^+$ m/z: 372.1050. found: 372.1051.

4.4.18. (E)-N-(2-(5-chloro-1H-indol-3-yl)ethyl)-2-((4-methylpyridin-2-yl)methylene)hydrazine-1-carbothioamide(5l)

Yellow solid, m. p. 207.7−209.6 °C, yield 71%. ^{1}H NMR (400 MHz, DMSO-d_6, ppm) δ 11.71 (s, 1H, −NH−), 11.06 (s, 1H, −NH−), 8.74 (t, J = 5.8 Hz, 1H, −NH−), 8.42 (s, J = 5.0 Hz, Ar−H), 8.11 (s, 1H, Ar−H), 7.98 (s, 1H, Ar−H), 7.78 (d, J = 1.5 Hz, 1H, Ar−H), 7.35 (dd, J = 15.6, 7.7 Hz, 1H, Ar−H), 7.30 (s, J = 1.8 Hz, 1H, −CH=N-), 7.21 (d, J = 4.8 Hz, 1H, Ar−H), 7.07 (dd, J = 8.6, 1.8 Hz, 1H, Ar−H), 3.84 (dd, J = 14.9, 6.4 Hz, 2H, −CH$_2$-), 3.11−2.92 (m, 2H, −CH$_2$-), 2.40 (d, J = 10.8 Hz, 3H, −CH$_3$). ^{13}C NMR (101 MHz, DMSO-d_6, δ, ppm) δ 177.13, 153.04, 149.06, 147.20, 142.46, 134.72, 128.47, 124.99, 124.60, 123.01, 122.75, 120.90, 120.43, 117.91, 112.87, 111.58, 44.35, 43.01, 24.74, 20.59. HR-MS (ESI), calcd. $C_{18}H_{18}ClN_5S$, [M+ Na]$^+$ m/z: 394.0869. found: 394.0867.

4.4.19. (E)-N-(2-(5-chloro-1H-indol-3-yl)ethyl)-2-((3-methylpyridin-2-yl)methylene)hydrazine-1-carbothioamide(5m)

White solid, m. p. 187.0−188.2 °C, yield 51%. ^{1}H NMR (400 MHz, DMSO-d_6, ppm) δ 11.65 (s, 1H, −NH−), 11.00 (s, 1H, −NH−), 8.65 (t, J = 5.8 Hz, 1H, −NH−), 7.94 (s, J = 37.1 Hz, 1H, Ar−H), 7.87 (d, J = 7.8 Hz, 1H, Ar−H), 7.76−7.58 (m, 2H, Ar−H), 7.35−7.27 (m, 1H, Ar−H), 7.23 (s, J = 4.8 Hz, 1H, −CH=N-), 7.17 (d, J = 7.5 Hz, 1H, Ar−H), 7.00 (dd, J = 8.6, 1.9 Hz, 1H, Ar−H), 3.75 (dd, J = 14.8, 6.4 Hz, 2H, −CH$_2$-), 3.01−2.87 (m, 2H, −CH$_2$-), 2.41 (s, 3H, −CH$_3$). ^{13}C NMR (100 MHz, DMSO-d_6, δ, ppm) δ 177.07, 157.67, 152.64, 142.43, 136.69, 134.71, 128.46, 124.64, 123.34, 123.03, 120.91, 117.85, 117.10, 112.89, 111.55, 44.34, 24.63, 23.79. HR-MS (ESI), calcd. $C_{18}H_{18}ClN_5S$, [M+ Na]$^+$ m/z: 394.0869. found: 394.0870.

4.4.20. (E)-N-(2-(5-chloro-1H-indol-3-yl)ethyl)-2-(1-(pyridin-2-yl)ethylidene)hydrazine-1-carbothioamide(5n)

Yellow solid, m. p. 182.2−183.7 °C, yield 61%. ^{1}H NMR (400 MHz, DMSO-d_6, ppm) δ 11.07 (d, J = 6.5 Hz, 1H, −NH−), 10.41 (s, 1H, −NH−), 8.70 (t, J = 5.8 Hz, 1H, NH-), 8.60 (t, J = 9.3 Hz, 1H, Ar−H), 8.17 (t, J = 19.6 Hz, 1H, Ar−H), 7.82 (dt, J = 13.4, 3.6 Hz, 1H, Ar−H), 7.79−7.70 (m, 1H, Ar−H), 7.46−7.36 (m, 2H, Ar−H), 7.30 (dd, J = 8.6, 2.0 Hz, 1H, Ar−H), 7.06 (dd, J = 8.6, 1.9 Hz, 1H, Ar−H), 3.82 (ddd, J = 42.8, 24.5, 17.3 Hz, 2H, −CH$_2$-), 3.02 (dd, J = 16.3, 8.9 Hz, 2H, −CH$_2$-), 2.39 (d, J = 7.8 Hz, 3H, −CH$_3$). ^{13}C NMR (100 MHz, DMSO-d_6, δ, ppm) δ 177.90, 154.68, 148.48, 148.08, 136.32, 134.76, 128.44, 124.68, 123.85, 123.05, 120.92, 120.53, 117.87, 112.88, 111.57, 44.40, 24.55, 12.16. HR-MS (ESI), calcd. $C_{18}H_{18}ClN_5S$, [M+H]$^+$ m/z: 372.1050. found: 372.1051.

4.4.21. (E)-N-(2-(5-chloro-1H-indol-3-yl)ethyl)-2-(1-(5-methylpyridin-2-yl)ethylidene)hydrazine-1-carbothioamide(5o)

Yellow solid, m. p. 190.3−191.6 °C, yield 53%. ^{1}H NMR (400 MHz, DMSO-d_6, ppm) δ 14.22 (s, 1H, −NH−), 11.05 (s, 1H, −NH−), 8.71 (t, J = 5.8 Hz, 1H, −NH−), 8.64 (d, J = 11.7 Hz, 1H, Ar−H), 7.96−7.83 (m, 1H, Ar−H), 7.76 (t, J = 2.8 Hz, 1H, Ar−H), 7.71−7.66 (m, 1H, Ar−H), 7.39−7.34 (m, 1H, Ar−H), 7.29 (d, J = 1.9 Hz, 1H, Ar−H), 7.07 (dd, J = 8.6, 1.9 Hz, 1H, Ar−H), 3.91−3.68 (m, 2H, −CH$_2$-), 3.06−2.88 (m, 2H, −CH$_2$-), 2.39 (d, J = 5.1 Hz, 3H, −CH$_3$), 2.34 (d, J = 5.6 Hz, 3H, −CH$_3$). ^{13}C NMR (100 MHz, DMSO-d_6, δ, ppm) δ 176.92, 149.79, 147.96, 138.40, 137.96, 134.71, 134.65, 128.46, 124.65, 124.11, 123.03, 120.88, 117.88, 112.86, 111.57, 44.36, 24.59, 21.85, 17.91. HR-MS (ESI), calcd. $C_{19}H_{20}ClN_5S$, [M+Na]$^+$ m/z: 408.1026. found: 408.1024.

4.4.22. (E)-N-(2-(1H-indol-3-yl)ethyl)-2-(1-(pyridin-2-yl)ethylidene)hydrazine-1-carbothioamide(5p)

Yellow solid, m. p. 147.8−149.7 °C, yield 85%. ^{1}H NMR (400 MHz, DMSO-d_6, ppm) δ 10.89 (s, 1H, −NH−), 10.43 (s, 1H, −NH−), 8.70 (s, 1H, −NH−), 8.59 (s, 1H, Ar−H), 8.21 (d, J = 7.5 Hz, 1H, Ar−H), 7.83 (d, J = 7.2 Hz, 1H, Ar−H), 7.75 (d, J = 7.3 Hz, 1H, Ar−H), 7.38 (s, 2H, Ar−H), 7.24 (s, 1H, Ar−H), 7.09 (s, 1H, Ar−H), 7.00 (s, 1H, Ar−H), 3.90 (d, J = 5.3 Hz, 2H, −CH$_2$-), 3.06 (s, 2H, −CH$_2$-), δ 2.40 (s, 3H, −CH$_3$). ^{13}C NMR (100 MHz, DMSO-d_6, δ, ppm) δ 178.51, 155.15, 148.90, 148.42, 136.86, 127.68, 124.37, 123.23, 121.52, 121.03, 119.09, 118.76, 112.01, 111.81, 44.90, 25.24, 12.66. HR-MS (ESI), calcd. $C_{18}H_{19}N_5S$, [M+H]$^+$ m/z: 338.1439. found: 338.1438.

4.4.23. (E)-N-(2-(1H-indol-3-yl)ethyl)-2-(1-(pyridin-2-yl)ethylidene)hydrazine-1-carbothioamide(5q)

Yellow solid, m. p. 186.6−187.5 °C, yield 72%. ^{1}H NMR (400 MHz, DMSO-d_6, ppm) δ 10.87 (s, 1H, −NH−), 10.34 (s, 1H, −NH−), 8.64 (t, J = 5.7 Hz, 1H, −NH−), 8.42 (s, 1H, Ar−H), 8.11 (d, J = 8.2 Hz, 1H, Ar−H), 7.74 (d, J = 7.8 Hz, 1H, Ar−H), 7.71−7.60 (m, 1H, Ar−H), 7.36 (t, J = 7.0 Hz, 1H, Ar−H), 7.22 (dd, J = 10.4, 2.1 Hz, 1H, Ar−H), 7.08 (t, J = 7.5 Hz, 1H, Ar−H), 6.99 (t, J = 7.4 Hz, 1H, Ar−H), 3.88 (dt, J = 19.8, 10.0 Hz, 2H, 2H, −CH$_2$-), 3.04 (dd, J = 16.7, 9.3 Hz, 2H, 2H, −CH$_2$-), 2.38 (s, 3H, −CH$_3$), 2.34 (s, 3H, −CH$_3$). ^{13}C NMR (100 MHz, DMSO-d_6, δ, ppm) δ 177.72, 152.13, 148.60, 148.12, 136.84, 136.31, 133.40, 127.21, 122.71, 121.01, 120.03, 118.60, 118.24, 111.43, 44.35, 24.76, 17.79, 12.14. HR-MS (ESI), calcd. $C_{17}H_{17}N_5S$, [M+Na]$^+$ m/z: 346.1102. found: 346.1108.

4.4.24. (E)-N-(2-(1H-indol-3-yl)ethyl)-2-(4-chlorobenzylidene)hydrazine-1-carbothioamide(5r)

White solid, m. p. 196.8−198.0 °C, yield 60%. ^{1}H NMR (400 MHz, DMSO-d_6, δ, ppm) δ 11.58 (s, 1H, −NH−), 10.86 (s, 1H, −NH−), 8.63 (t, J = 5.7 Hz, 1H, −NH−), 8.04 (s, 1H, Ar−H), 7.75 (dd, J = 22.1, 8.2 Hz, 3H, Ar−H), 7.49 (d, J = 8.5 Hz, 2H, Ar−H), 7.36 (d, J = 8.1 Hz, 1H, Ar−H), 7.22 (s, J = 2.1 Hz, 1H, −CH=N−), 7.08 (dd, J = 11.1, 4.0 Hz, 1H, Ar−H), 6.99 (dd, J = 10.9, 4.0 Hz, 1H, Ar−H), 3.84 (dd, J = 14.9, 6.3 Hz, 2H, −CH$_2$-), 3.13−2.98 (m, 2H, −CH$_2$-). ^{13}C NMR (101 MHz, DMSO-d_6, δ, ppm) δ 176.90, 140.38, 136.28, 134.15, 133.17, 128.77, 128.71, 127.24, 122.66, 120.99, 118.55, 118.24, 111.53, 111.36, 44.26, 24.85. HR-MS (ESI), calcd. $C_{18}H_{17}ClN_4S$, [M+H]$^+$ m/z: 357.0940. found: 357.0939.

4.4.25. (E)-N-(2-(1H-indol-3-yl)ethyl)-2-(4-methylbenzylidene)hydrazine-1-carbothioamide(5s)

White solid, m. p. 119.1−120.6 °C, yield 59%. ^{1}H NMR (400 MHz, DMSO-d_6, δ, ppm) δ 11.45 (s, 1H, −NH−), 10.86 (s, 1H, −NH−), 8.53 (t, J = 5.8 Hz, 1H, −NH−), 8.02 (s, 1H, Ar−H), 7.73 (d, J = 7.8 Hz, 1H, Ar−H), 7.63 (d, J = 8.1 Hz, 2H, Ar−H), 7.35 (d, J = 8.1 Hz, 1H, Ar−H), 7.23 (dd, J = 10.8, 5.0 Hz, 3H, 2Ar−H, 1-CH=N-), 7.08 (t, J = 7.1 Hz, 1H, Ar−H), 6.99 (t, J = 7.4 Hz, 1H, Ar−H), 3.83 (dd, J = 14.9, 6.3 Hz, 2H, −CH$_2$-), 3.08−2.96 (m, 2H, −CH$_2$-), 2.34 (s, 3H, −CH$_3$). ^{13}C NMR

(100 MHz, DMSO-d_6, δ, ppm) δ 176.74, 141.91, 139.55, 136.27, 131.44, 129.27, 127.25, 127.13, 122.64, 120.97, 118.57, 118.22, 111.58, 111.35, 44.25, 24.91, 21.02. HR-MS (ESI), calcd. $C_{19}H_{20}N_4S$, $[M+H]^+$ m/z: 337.1487. found: 337.1486.

4.4.26. (E)-N-(2-(1H-indol-3-yl)ethyl)-2-benzylidenehydrazine-1-carbothioamide(5t)

White solid, m. p. 213.7−215.9 °C, yield 63%. ^1H NMR (400 MHz, DMSO-d_6, δ, ppm) δ 11.52 (s, 1H, −NH−), 10.86 (s, 1H, −NH−), 8.58 (t, J = 5.7 Hz, 1H, −NH−), 8.06 (s, 1H, Ar−H), 7.74 (dd, J = 7.6, 4.7 Hz, 3H, Ar−H), 7.51−7.31 (m, 4H, Ar−H), 7.22 (s, J = 1.8 Hz, 1H, −CH=N−), 7.08 (t, J = 7.5 Hz, 1H, Ar−H), 6.99 (t, J = 7.4 Hz, 1H, Ar−H), 3.84 (dd, J = 14.7, 6.4 Hz, 2H, −CH$_2$-), 3.12−2.95 (m, 2H, −CH$_2$-). ^{13}C NMR (101 MHz, DMSO-d_6, δ, ppm) δ 176.87, 141.78, 136.27, 134.16, 129.75, 128.65, 127.26, 127.14, 122.65, 120.98, 118.56, 118.24, 111.57, 111.35, 44.29, 24.88. HR-MS (ESI), calcd. $C_{18}H_{18}N_4S$, $[M+H]^+$ m/z: 323.1330. found: 323.1329.

4.4.27. (E)-N-(2-(1H-indol-3-yl)ethyl)-2-(1-(p-tolyl)ethylidene) hydrazine-1-carbothioamide(5u)

White solid, m. p. 190.9−191.7 °C, yield 53%. ^1H NMR (400 MHz, DMSO-d_6, δ, ppm) δ 10.87 (s, 1H, −NH−), 10.22 (s, 1H, −NH−), 8.47 (t, J = 5.7 Hz, 1H, −NH−), 7.77−7.64 (m, 3H, Ar−H), 7.36 (d, J = 8.1 Hz, 1H, Ar−H), 7.22 (dd, J = 5.2, 2.7 Hz, 3H, Ar−H), 7.13−7.02 (m, 1H, Ar−H), 7.03−6.91 (m, 1H, Ar−H), 3.87 (dd, J = 14.4, 6.4 Hz, 2H, −CH$_2$-), 3.10−2.95 (m, 2H, −CH$_2$-), 2.34 (s, 3H, −CH$_3$), 2.27 (s, 3H, −CH$_3$). ^{13}C NMR (100 MHz, DMSO-d_6, δ, ppm) δ 177.68, 147.70, 138.77, 136.33, 134.82, 128.87, 127.20, 126.36, 122.71, 121.00, 118.61, 118.23, 111.52, 111.36, 44.23, 24.82, 20.85, 13.96. HR-MS (ESI), calcd. $C_{20}H_{22}N_4S$, $[M+H]^+$ m/z: 351.1643. found: 351.1643.

4.4.28. (E)-N-(2-(1H-indol-3-yl)ethyl)-2-(1-(4-chlorophenyl) ethylidene)hydrazine-1-carbothioamide(5v)

White solid, m. p. 176.6−178.2 °C, yield 58%. ^1H NMR (400 MHz, DMSO-d_6, δ, ppm) δ 10.87 (s, 1H, −NH−), 10.33 (s, 1H, −NH−), 8.51 (t, J = 5.6 Hz, 1H, −NH−), 7.84 (d, J = 8.7 Hz, 2H, Ar−H), 7.72 (d, J = 7.8 Hz, 1H, Ar−H), 7.46 (d, J = 8.7 Hz, 2H, Ar−H), 7.36 (d, J = 8.1 Hz, 1H, Ar−H), 7.23 (d, J = 2.1 Hz, 1H, Ar−H), 7.07 (dd, J = 11.1, 3.9 Hz, 1H, Ar−H), 6.98 (dd, J = 10.9, 3.9 Hz, 1H, Ar−H), 3.87 (dd, J = 14.2, 6.5 Hz, 2H, −CH$_2$-), 3.04 (t, J = 7.5 Hz, 2H, −CH$_2$-), 2.29 (s, 3H, −CH$_3$). ^{13}C NMR (100 MHz, DMSO-d_6, δ, ppm) δ 177.79, 146.33, 136.47, 136.34, 133.85, 128.23, 128.18, 127.19, 122.75, 121.01, 118.59, 118.24, 111.48, 111.36, 44.24, 40.14, 39.93, 39.72, 39.52, 39.31, 39.10, 38.89, 24.75, 13.91. HR-MS (ESI), calcd. $C_{19}H_{19}ClN_4S$, $[M+H]^+$ m/z: 371.1097. found: 371.1098.

4.5. Cell culture and reagents

Human prostate cancer cells (PC3), gastric cancer cells (MGC803), esophageal cancer cells (EC109), human gastric mucosal epithelial cells (GES-1) and human normal prostate cell (WPMY-1) were obtained from our laboratories (originally purchased from the CCTCC). RPMI 1640 medium was bought from Solarbio. Fetal Bovine Serum (FBS) was purchased from Bioind (BI). All cancer cells were cultured in RPMI 1640 medium with 10% FBS and all cancer cells were cultured in a humidified incubator of 95% air and 5% CO_2 at 37 °C. Compounds were dissolved in DMSO at an initial concentration of 10 mM. Hoechst 33342 was purchased from Beyotime Biotechnology. PI and RNase A were purchased from Solarbio. Annexin V-FITC/PI Apoptosis Detection Kit was bought from Keygen Biotech. The antibodies used in western blotting are as follows: Bax (#505992, Proteintech), Bcl-2 (#15071T, CST), P53 (2527T, CST), Caspase9 (9508T, CST), Cleaved caspase 3 (9664T, CST), PARP (9532T, CST), GAPDH (AB-P-R001, Good Here Technology).

4.6. Cell viability assay

Cells in the experimental growth phase were seeded in 96-well plates at approximately 3.8−5.0 × 10^3 cells per well. Incubate for approximately 24 h, then removed the medium and added 200 μl fresh medium with different concentrations of compound 5j per well. After 24 h, 48 h, 72 h incubation, 20 μl of MTT (3-(4,5-dimethylthiazol-2-yl)-2,5-diphenyltetrazolium bromide) solution (5 mg/ml) was added to each well, and cells were incubated at 37 °C for 4 h in the dark. Then, the medium was removed, added 150 μl DMSO, and was shaken on the shaker for about 10−15 min until the formazan dissolved completely. The absorbance was measures at 490 nm with a microplate reader. The date of IC$_{50}$ was calculated using SPASS 17.0 software, and the cell viability curve of compound 5j was obtained by GraphPad Prism 5.0 software.

4.7. Colony formation assay

Cells in the exponential growth phase were seeded in 6-well plate at a concentration of 1.1 × 10^3 per well. After approximately 24 h incubation, added 2 ml fresh medium with different concentrations of compound 5j per well, and incubated for 7 days. After washing 2−3 times with PBS, cells were fixed with methanol (4 °C pre-cooling) for 1 h and stained with crystal violet for 1 h. After that, images were photographed after drying the plate. The crystals were dissolved in 33% acetic acid for 30 min. The absorbance was measured at 570 nm with a microplate reader.

4.8. Cell cycle analysis

PC3 cells were seeded in 6-well plates at a concentration of 2.5 × 10^5 per well. After 24 h incubation, treated with various concentrations of compound 5j for 48 h or 72 h. After that, collected cells, fixed with pre-cooled 70% ethanol at −20 °C overnight and stained with 20 μg/ml PI and 20 μg/ml RNase A. Before analyzed by flow cytometer (BD Bioscience, USA), the cells were protected from light for 30 min. Flowjo 7.6 software was used to analyze the date of cell cycle.

4.9. Wound healing assay

The cell migration ability was evaluated by wound healing assay. PC3 cells were seeded in 6-well plates at a concentration of 3.5 × 10^5 per well. Until the cells density reached 90%−95%, the cell surface was scratched by a 200 μl pipet tip. Next, the cells were washed three or four times with PBS and added fresh medium with 1% FBS and different concentrations of compound 5j. After 48 h incubation, images were photographed using an inverted microscope.

4.10. Transwell assay

Cells were first starved with serum-free medium for 12 h and then harvested with trypsin. Cells were seeded in transwell 24-well plate at a concentration of 3 × 10^5 per well. 20% FBS and compound 5j was added in the lower chamber, and compound 5j was added in the upper chamber with no serum. After incubation for 48 h, removed the medium and washed twice with PBS. Then, the cells were fixed with pre-cooled methanol for 1 h at 4 °C, stained with crystal violet for 30 min at room temperature, and photographed using upright microscope. The date of cell number was analyzed by ImageJ software.

4.11. Hoechst 33342 staining

Cells were seeded in 24-well plates at a concentration of 5×10^4 per well. After 24 h incubation, added 500 μl fresh medium containing different concentrations of compound **5j** for another 72 h. Then, added Hoechst 33342 (100×) 5 μl per well and stained in the dark for 45 min. After that, the cells were washed twice with PBS and photographed by fluorescence microscopy under UV excitation.

4.12. Analysis of apoptosis by flow cytometry

Cells were seeded in 6-well plates at a concentration of 2×10^5 per well. After 24 h incubation, the cells were treated with different concentrations of compound **5j** for 72 h. The cells were harvested with trypsin, washed with PBS and used Annexin V-FITC/PI apoptosis Kit according to the protocol. Then, the cells were detected using the flow cytometry (BD Bioscience, USA). The date of apoptosis was analyzed by the Flowjo 7.6 software. Apoptosis (%) = early apoptosis (%) + late apoptosis (%).

4.13. Western analysis

Cells were seeded in cell culture dishes (100 mm). After 24 h incubation, the cells were treated with different concentrations of compound **5j** for 72 h. Then, the cells were harvested with trypsin and lysed with cell/tissue RIPA lysis buffer (RIPA, 1% PMSF, 1% total enzyme inhibitor, 1% phosphatase inhibitor) for 30 min. The protein was quantified by BCA Kit according to the protocol and denatured in water at 100 °C for 10 min. After that, protein was separated by 10%−15% SDS-PAGE, and transferred to nitrocellulose membrane. The nitrocellulose membrane was blocked with PBST containing 5% nonfat milk for 1−2 h at room temperature and incubated with primary antibody (1:1000) overnight at 4 °C, followed by incubation with secondary antibody (1:10000) for 2 h at room temperature. The immunoblots were examined by enhanced chemiluminescence Kit.

Appendix A. Supplementary data

Supplementary data to this article can be found online at https://doi.org/10.1016/j.ejmech.2019.111764.

References

[1] J. Zhang, S.S. Spath, S.L. Marjani, W. Zhang, Characterization of cancer genomic heterogeneity by next-generation sequencing advances precision medicine in cancer treatment, Precis. Clin. Med. 1 (2018) 29−48.
[2] Y. Hou, L. Zhu, Z. Li, Q. Shen, Q. Xu, W. Li, Y. Liu, P. Gong, Design, synthesis and biological evaluation of novel 7-amino-[1,2,4]triazolo[4,3-f]pteridinone, and 7-aminotetrazolo[1,5-f]pteridinone derivative as potent antitumor agents, Eur. J. Med. Chem. 163 (2019) 690−709.
[3] C.R. Nishida, P.R. Ortiz de Montellano, Bioactivation of antituberculosis thioamide and thiourea prodrugs by bacterial and mammalian flavin monooxygenases, Chem. Biol. Interact. 192 (2011) 21−25.
[4] B. Sarkanj, M. Molnar, M. Cacic, L. Gille, 4-Methyl-7-hydroxycoumarin antifungal and antioxidant activity enhancement by substitution with thiosemicarbazide and thiazolidinone moieties, Food Chem. 139 (2013) 488−495.
[5] V.F. Pape, S. Toth, A. Furedi, K. Szebenyi, A. Lovrics, P. Szabo, M. Wiese, G. Szakacs, Design, synthesis and biological evaluation of thiosemicarbazones, hydrazinobenzothiazoles and arylhydrazones as anticancer agents with a potential to overcome multidrug resistance, Eur. J. Med. Chem. 117 (2016) 335−354.
[6] H.K.a.M. Gupta*, Recent advances in thiosemicarbazones as anticancer agents, Int. J. Pharm. Chem. Biol. Sci. 8 (2018) 259−265.
[7] P. Heffeter, V.F.S. Pape, E.A. Enyedy, B.K. Keppler, G. Szakacs, C.R. Kowol, Anticancer thiosemicarbazones: chemical properties, interaction with iron metabolism, and resistance development, Antioxidants Redox Signal. 30 (2019) 1062−1082.
[8] K.L. Summers, A structural chemistry perspective on the antimalarial properties of thiosemicarbazone metal complexes, Mini Rev. Med. Chem. 19 (2019) 569−590.
[9] L.Y. Ma, Y.C. Zheng, S.Q. Wang, B. Wang, Z.R. Wang, L.P. Pang, M. Zhang, J.W. Wang, L. Ding, J. Li, C. Wang, B. Hu, Y. Liu, X.D. Zhang, J.J. Wang, Z.J. Wang, W. Zhao, H.M. Liu, Design, synthesis, and structure-activity relationship of novel LSD1 inhibitors based on pyrimidine-thiourea hybrids as potent, orally active antitumor agents, J. Med. Chem. 58 (2015) 1705−1716.
[10] E.N. Parker, J. Song, G.D. Kishore Kumar, S.O. Odutola, G.E. Chavarria, A.K. Charlton-Sevcik, T.E. Strecker, A.L. Barnes, D.R. Sudhan, Synthesis and biochemical evaluation of benzoylbenzophenone thiosemicarbazone analogues as potent and selective inhibitors of cathepsin L, Bioorg. Med. Chem. 23 (2015) 6974−6992.
[11] H.E. Elsayed, H.Y. Ebrahim, E.G. Haggag, A.M. Kamal, K.A. El Sayed, Rationally designed hecogenin thiosemicarbazone analogs as novel MEK inhibitors for the control of breast malignancies, Bioorg. Med. Chem. 25 (2017) 6297−6312.
[12] Y. Yu, J. Wong, D.B. Lovejoy, D.S. Kalinowski, D.R. Richardson, Chelators at the cancer coalface: desferrioxamine to Triapine and beyond, Clin. Cancer Res. 12 (2006) 6876−6883.
[13] B.M. Zeglis, V. Divilov, J.S. Lewis, Role of metalation in the topoisomerase IIalpha inhibition and antiproliferation activity of a series of alpha-heterocyclic-N4-substituted thiosemicarbazones and their Cu(II) complexes, J. Med. Chem. 54 (2011) 2391−2398.
[14] M.L. Pati, M. Niso, D. Spitzer, F. Berardi, M. Contino, C. Riganti, W.G. Hawkins, C. Abate, Multifunctional thiosemicarbazones and deconstructed analogues as a strategy to study the involvement of metal chelation, Sigma-2 (sigma 2) receptor and P-gp protein in the cytotoxic action: in vitro and in vivo activity in pancreatic tumors, Eur. J. Med. Chem. 144 (2018) 359−371.
[15] M.S.L. Zhi-Gang Jiang, Hossein A. Ghanbari, Neuroprotective activity of 3-aminopyridine-2-carboxaldehyde thiosemicarbazone (PAN-811), a cancer therapeutic agent, CNS Drug Rev. 12 (2006) 77−90.
[16] a Anna Mrozek-Wilczkiewicz, a Katarzyna Malarz, b Marta Rejmund, b Jaroslaw Polanski, Robert Musiol, Anticancer activity of the thiosemicarbazones that are based on di-2 pyridine ketone and quinoline moiety, Eur. J. Med. Chem. 171 (2019) 180−194.
[17] B. Hu, B. Wang, B. Zhao, Q. Guo, Z.H. Li, X.H. Zhang, G.Y. Liu, Y. Liu, Y. Tang, F. Luo, Y. Du, Y.X. Chen, L.Y. Ma, H.M. Liu, Thiosemicarbazone-based selective proliferation inactivators inhibit gastric cancer cell growth, invasion, and migration, Medchemcomm 8 (2017) 2173−2180.
[18] W.-C.H.H.-C. CHANG, Indole-3-carbinol inhibits sp1-induced matrix metalloproteinase-2 expression to attenuate migration and invasion of breast cancer cells, J. Agric. Food Chem. 57 (2009) 76−82.
[19] J.N. Ho, W. Jun, R. Choue, J. Lee, I3C and ICZ inhibit migration by suppressing the EMT process and FAK expression in breast cancer cells, Mol. Med. Rep. 7 (2013) 384−388.
[20] C. Sherer, T.J. Snape, Heterocyclic scaffolds as promising anticancer agents against tumours of the central nervous system: exploring the scope of indole and carbazole derivatives, Eur. J. Med. Chem. 97 (2015) 552−560.
[21] M.S. Mady, M.M. Mohyeldin, H.Y. Ebrahim, H.E. Elsayed, W.E. Houssen, E.G. Haggag, R.F. Soliman, K.A. El Sayed, The indole alkaloid meleagrin, from the olive tree endophytic fungus Penicillium chrysogenum, as a novel lead for the control of c-Met-dependent breast cancer proliferation, migration and invasion, Bioorg. Med. Chem. 24 (2016) 113−122.
[22] S. Dadashpour, S. Emami, Indole in the target-based design of anticancer agents: a versatile scaffold with diverse mechanisms, Eur. J. Med. Chem. 150 (2018) 9−29.
[23] N. Fortunati, F. Marano, A. Bandino, R. Frairia, M.G. Catalano, G. Boccuzzi, The pan-histone deacetylase inhibitor LBH589 (panobinostat) alters the invasive breast cancer cell phenotype, Int. J. Oncol. 44 (2014) 700−708.
[24] G. Qin, Y. Li, X. Xu, X. Wang, K. Zhang, Y. Tang, H. Qiu, D. Shi, C. Zhang, Q. Long, Panobinostat (LBH589) inhibits Wnt/beta-catenin signaling pathway via upregulating APCL expression in breast cancer, Cell. Signal. 59 (2019) 62−75.
[25] T. Kim, Y.J. Kim, I.H. Han, D. Lee, J. Ham, K.S. Kang, J.W. Lee, The synthesis of sulforaphane analogues and their protection effect against cisplatin induced cytotoxicity in kidney cells, Bioorg. Med. Chem. Lett 25 (2015) 62−66.
[26] C.-y.D. Yu-peng Tian, Cun-yuan zhao, and xiao-zeng you*, synthesis, crystal structure, and second-order optical nonlinearity, inorg. Chem. 36 (1997) 1247−1252.
[27] b. El Sayed H. El Ashrya, Sammer Yousufa*, H. Hayat, c Hassana, Magdy K. Zahranc, Ali S. Hebishyc, Synthesis and single-crystal X-ray diffraction studies ofan arylidenethiosemica, Lett. Org. Chem. 11 (2014) 101−108.
[28] J.F. de Oliveira, T.S. Lima, D.B. Vendramini-Costa, S.C.B. de Lacerda Pedrosa,

E.A. Lafayette, R.M.F. da Silva, S.M.V. de Almeida, R.O. de Moura, A. Ruiz, J.E. de Carvalho, M. de Lima, Thiosemicarbazones and 4-thiazolidinones indole-based derivatives: synthesis, evaluation of antiproliferative activity, cell death mechanisms and topoisomerase inhibition assay, Eur. J. Med. Chem. 136 (2017) 305−314.

[29] J.L. de Melos, E.C. Torres-Santos, S. Faioes Vdos, N. Del Cistia Cde, C.M. Sant'Anna, C.E. Rodrigues-Santos, A. Echevarria, Novel 3,4-methylenedioxyde-6-X-benzaldehyde-thiosemicarbazones: synthesis and antileishmanial effects against Leishmania amazonensis, Eur. J. Med. Chem. 103 (2015) 409−417.

[30] M.G. Temraz, P.A. Elzahhar, A.B.A. El-Din, A.A. Bekhit, H.F. Labib, A.S.F. Belal, Anti-leishmanial click modifiable thiosemicarbazones: design, synthesis, biological evaluation and in silico studies, Eur. J. Med. Chem. 151 (2018) 585−600.

[31] Z. Liu, S. Wu, Y. Wang, R. Li, J. Wang, L. Wang, Y. Zhao, P. Gong, Design, synthesis and biological evaluation of novel thieno[3,2-d]pyrimidine de-rivatives possessing diaryl semicarbazone scaffolds as potent antitumor agents, Eur. J. Med. Chem. 87 (2014) 782−793.

[32] J.F. de Oliveira, A.L. da Silva, D.B. Vendramini-Costa, C.A. da Cruz Amorim, J.F. Campos, A.G. Ribeiro, R. Olimpio de Moura, J.L. Neves, A.L. Ruiz, J. Ernesto de Carvalho, C. Alves de Lima Mdo, Synthesis of thiophene-thiosemicarbazone derivatives and evaluation of their in vitro and in vivo antitumor activities, Eur. J. Med. Chem. 104 (2015) 148−156.

[33] P. Chellan, N. Shunmoogam-Gounden, D.T. Hendricks, J. Gut, P.J. Rosenthal, C. Lategan, P.J. Smith, K. Chibale, G.S. Smith, Synthesis, structure and in vitro biological screening of palladium(II) complexes of functionalised salicylaldi-mine thiosemicarbazones as antimalarial and anticancer agents, Eur. J. Inorg. Chem. 2010 (2010) 3520−3528.

[34] F. Vandresen, H. Falzirolli, S.A. Almeida Batista, A.P. da Silva-Giardini, D.N. de Oliveira, R.R. Catharino, A.L. Ruiz, J.E. de Carvalho, M.A. Foglio, C.C. da Silva, Novel R-(+)-limonene-based thiosemicarbazones and their antitumor activity against human tumor cell lines, Eur. J. Med. Chem. 79 (2014) 110−116.

[35] Z.H. Li, J. Zhang, X.Q. Liu, P.F. Geng, J.L. Ma, B. Wang, T.Q. Zhao, B. Zhao, H.M. Wei, C. Wang, D.J. Fu, B. Yu, H.M. Liu, Identification of thiazolo[5,4-d] pyrimidine derivatives as potent antiproliferative agents through the drug repurposing strategy, Eur. J. Med. Chem. 135 (2017) 204−212.

[36] C. Wang, L. Jiang, S. Wang, H. Shi, J. Wang, R. Wang, Y. Li, Y. Dou, Y. Liu, G. Hou, Y. Ke, H. Liu, The antitumor activity of the novel compound jesridonin on human esophageal carcinoma cells, PLoS One 10 (2015) 1−23.

[37] A.L. Grilo, A. Mantalaris, Apoptosis: a mammalian cell bioprocessing perspective, Biotechnol. Adv. 37 (2019) 459−475.

[38] L. Ouyang, Z. Shi, S. Zhao, F.T. Wang, T.T. Zhou, B. Liu, J.K. Bao, Programmed cell death pathways in cancer: a review of apoptosis, autophagy and programmed necrosis, Cell Prolif 45 (2012) 487−498.

[39] I.C. Etti, A. Rasedee, N.M. Hashim, A.B. Abdul, A. Kadir, S.K. Yeap, P. Waziri, I. Malami, K.L. Lim, C.J. Etti, Artonin E induces p53-independent G1 cell cycle arrest and apoptosis through ROS-mediated mitochondrial pathway and livin suppression in MCF-7 cells, Drug Des. Dev. Ther. 11 (2017) 865−879.

[40] J.J. Rodgers, R. McClure, M.R. Epis, R.J. Cohen, P.J. Leedman, J.M. Harvey, B. Australian Prostate Cancer, M.A. Thomas, J.M. Bentel, ETS1 induces trans-forming growth factor beta signaling and promotes epithelial-to-mesenchymal transition in prostate cancer cells, J. Cell. Biochem. 120 (2019) 848−860.

[41] Q. Cheng, Y.J. Shi, Z. Li, H. Kang, Z. Xiang, L.F. Kong, FAST1 promotes the migration and invasion of colorectal cancer cells, Biochem. Biophys. Res. Commun. 509 (2019) 407−413.

[42] R. Jan, G.E. Chaudhry, Understanding apoptosis and apoptotic pathways tar-geted cancer therapeutics, Adv. Pharmaceut. Bull. 9 (2019) 205−218.